Quaternary International 253 (2012) 32–46

Contents lists available at ScienceDirect

Quaternary International

journal homepage: www.elsevier.com/locate/quaint

Have the Southern Westerlies changed in a zonally symmetric manner over the last 14,000 years? A hemisphere-wide take on a controversial problem

Michael-Shawn Fletcher [a,*], Patricio Iván Moreno [a,b]

[a] Institute of Ecology and Biodiversity, University of Chile, Santiago, Chile
[b] Department of Ecological Sciences, University of Chile, Santiago, Chile

ARTICLE INFO

Article history:
Available online 10 May 2011

ABSTRACT

The prevailing view in the palaeoclimate literature of the last 20 years is that the Southern Westerly Winds (SWW) were intensified over southern Australia and Tasmania during the warmer-than-present early Holocene (11–8 ka). At similar latitudes on the opposite side of the southern mid-latitudes, palaeoclimate studies have suggested a poleward shift of the northern edge of the westerlies and focusing at 49°S in southern South America. This zonal asymmetry contrasts with the modern day zonal symmetry displayed by the SWW and poses a formidable challenge to an understanding of the modes of climatic variability of the southern extra-tropics. This paper presents an updated synthesis of continuous, radiocarbon-dated palaeoenvironmental data from the westerlies zone of influence in all Southern Hemisphere continents. Synchronous multi-millennial trends in moisture, vegetation, fire, and hydrologic balance are remarkably consistent with the way the SWW changes impact upon the climate in Southern Hemisphere landmasses in the modern climate. Considering the modern relationships between local precipitation and zonal wind speeds, it is suggested that the SWW changed in a zonally symmetric manner at multi-millennial scale between 14 and 5 ka. Regional asymmetry develops after 5 ka across the Southern Hemisphere, with a pattern of precipitation anomalies akin to the modern functioning of El Niño – Southern Oscillation, which started ~6200 years ago.

1. Introduction

The absence of major topographic barriers in the Southern Hemisphere middle latitudes allows the development of strongly zonal atmospheric and oceanic circulation patterns, i.e. the Southern Westerly Winds (SWW) and the Antarctic Circum-Polar Current. The modern Southern Westerly Winds are a strikingly symmetric component of the climate system that dictate the climate of all Southern Hemisphere landmasses south of ~30°S (Garreaud, 2007), and also govern nutrient, heat, and gas fluxes between surface and deep oceanic water masses in the Southern Ocean and the atmosphere.

Recent research has led to the realisation that the SWW may have played a key role in the generation of past atmospheric CO_2 variations, establishing a conduit for inter-hemispheric propagation of palaeoclimate signals during ice-age terminations (Toggweiler et al., 2006; Anderson et al., 2009; Toggweiler, 2009; Denton et al., 2010) and the Holocene (Moreno et al., 2010; Fletcher and Moreno, 2011). Despite this importance, there are few chronologies of past variations of the SWW that span their entire zone of influence during and since the Last Glacial Maximum (LGM). The current understanding relies on local, regional and sub-continental scale palaeoenvironmental reconstructions (e.g. Markgraf et al., 1992; Harrison, 1993; Shulmeister et al., 2004; Gilli et al., 2005a, b; Moreno et al., 2010) and meridionally aligned transects (e.g. Markgraf et al., 2000; Ono et al., 2004; Turney et al., 2006a), with little attempt to integrate data from across the entire westerly wind zone of influence (Heusser, 1989a). As a consequence, understanding of hemisphere-wide westerly change through the Quaternary in the Southern Hemisphere is largely piecemeal, often contradictory and is the source of considerable discussion in the palaeoclimate literature (Heusser, 1989a, b; Markgraf, 1989; Markgraf et al., 1992; Harrison and Dodson, 1993; Dodson, 1998; Shulmeister, 1999; Shulmeister et al., 2004; Lamy et al., 2010; Moreno et al., 2010; Fletcher and Moreno, 2011).

Controversy and debate are inevitable products of scientific endeavour and, indeed, it could be argued that the basic tenet of falsification encourages researchers to entertain controversial, or, perhaps more correctly, adversarial positions in order to produce

* Corresponding author.
E-mail addresses: michael.fletcher@u.uchile.cl, michael.fletcher@live.com.au (M.-S. Fletcher).

1040-6182/$ – see front matter © 2011 Elsevier Ltd and INQUA. All rights reserved.
doi:10.1016/j.quaint.2011.04.042

robust scientific theory. Perhaps the most visible controversy pertaining to the SWW through the Quaternary regards their behaviour during the Last Glacial Maximum (LGM). The opposing camps in the palaeoclimate literature argue for either a southerly/poleward displacement (e.g. Markgraf, 1987, 1989; Markgraf et al., 1992; Harrison and Dodson, 1993; Markgraf, 1993; Dodson, 1998); a northerly/equatorward displacement (e.g. Nicholson and Flohn, 1980; Heusser, 1989b; Lamy et al., 1999; Moreno et al., 1999; Holmgren et al., 2003; Ono et al., 2004; Shulmeister et al., 2004; Fletcher and Thomas, 2010b); or little, if any, change of the mean latitudinal position of the SWW relative to today (Wyrwoll et al., 2000; Hesse et al., 2004; Rojas et al., 2009). To date, this issue is still a matter of discussion and consensus remains elusive.

A less adversarial, but not less contentious issue prevails between models of SWW change through the late Pleistocene and Holocene. During the early Holocene interval (ca. 11,000–8000 cal ka), for example, arguments exist for both a northward displacement and/or strengthening of the westerlies in southern South America (west of the Andes around 30°S) (Veit, 1996) and Australia (e.g. Harrison and Dodson, 1993; Dodson, 1998; Gingele et al., 2007; Moros et al., 2009); and a southward displacement and/or weakening of the SWW in southwest South America (below 32°S) (Jenny et al., 2003; Moreno and Leon, 2003; Moreno, 2004; Villa-Martinez and Moreno, 2007; Lamy et al., 2010; Moreno et al., 2010), New Zealand (Shulmeister, 1999; McGlone et al., 2000; Shulmeister et al., 2004), Africa (Holmgren et al., 2003) and Australia (Shulmeister, 1999). The mid Holocene (ca. 7–5 ka) is equally contradictory, with arguments for a northward displacement and/or increased intensity of westerly flow (relative to the early Holocene ca. 11–7 ka) in southern South America (Jenny et al., 2003; Moreno, 2004; Moreno et al., 2010), New Zealand (Shulmeister et al., 2004), Australia (Shulmeister, 1999; Fletcher and Thomas, 2010b) and Africa (Holmgren et al., 2003); and a southward displacement and/or weaker intensity of westerly flow (relative to the early Holocene) in Australia (Harrison and Dodson, 1993; Moros et al., 2009) and Africa (Nicholson and Flohn, 1980). Accordingly, it is not possible to draw a clear conclusion from the palaeoclimate literature as to whether changes in the SWW during or since the LGM have been zonally symmetric, nor is it possible to draw consensus on the direction of westerly change. The lack of resolve over the behaviour of the SWW through the last glacial–interglacial cycle is, given their importance in regional and global climate systems, an Achilles Heel to attempts at understanding and predicting regional and global climate dynamics.

A basic premise in these studies is the correlation between local precipitation and zonal wind speeds, which holds true for several parts of the southern mid-latitudes in the modern climate (Fig. 1) and which is important in a palaeoclimatic context, as it suggests that palaeohydrological reconstructions from regions within the Southern Westerly zone of influence may proxy relative westerly wind influence. A complicating factor in the interpretation of palaeohydrological changes, though, is that this relationship may have changed its strength or sign in some regions since the LGM, or that other moisture sources not as important in the modern hydrologic balance could have had more importance in the past. Identifying these non-stationarities require an array of detailed records, unavailable for most regions today.

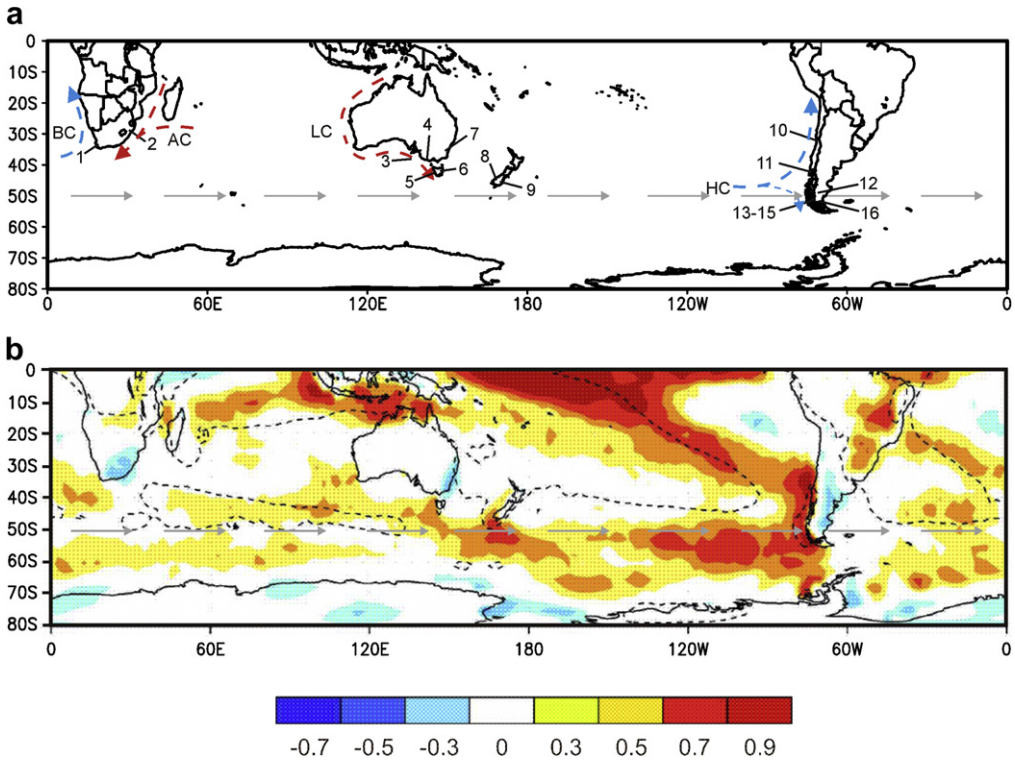

Fig. 1. Maps showing (a) the location of sites and boundary currents mentioned in the text and (b) the local correlation between zonal wind strength and precipitation from the equator to 80°S (scale bar indicates the strength of correlation; Garreaud, 2007). BC – Benguela Current; AC – Agulhas Current; LC – Leeuwin Current; HC – Humboldt Current. Note the anti-phased precipitation response to westerly wind speed between west facing and east facing coasts in all Southern Hemisphere landmasses. The grey arrows indicate the approximate latitude of maximum westerly wind speed (50°S). Site list: 1 – Western Cape region of South Africa; 2 – Mataputaland, South Africa; 3 – ocean core MD03-2611; 4 – Southwest Victoria, Australia; 5 – Western Tasmania, Australia; 6 – Eastern Tasmania, Australia; 7 – Lake George, southeast Australia; 8 – Okarito Bog, South Island, New Zealand; 9 – Otago, South Island, New Zealand; 10 – Laguna Acuelo, Chile; 11 – Lago Condorito, Chile; 12 – Lago Cardiel, Argentina; 13 – Lago Guanaco, Chile; 14 – Lago Tamar, Chile; 15 – Gran Campo-2, Chile; 16 – Laguna Potrok Aike, Argentina.

This paper synthesises and analyses palaeoenvironmental data from areas located within the SWW zone of influence in Africa, southern Australia, New Zealand and southern South America (Fig. 1a). It specifically aims to address the following questions: (1) are coherent, multi-millennial scale changes in the SWW inferable from palaeoenvironmental data?; (2) are multi-millennial scale changes in palaeohydrology in Southern Hemisphere landmasses consistent with the modern relationship between westerly wind speed and precipitation?; (3) have multi-millennial scale changes in the Southern Westerlies been zonally symmetric over the last 14,000 years?; and (4) how relevant are SWW changes for understanding variations in the CO_2 content of the atmosphere during and since the LGM?

2. Southern Australia

2.1. Present environment

The climate of Australia is dominated by the sub-tropical high pressure system associated with the cool and dry descending air of the Hadley Cell (Sturman and Tapper, 2006). In the south of Australia, the sub-tropical high pressure system interacts with the SWW and an increasingly cooler winter rain climate prevails toward the south. On west facing coasts in southern Australia (e.g. southwest Victoria and southwest Western Australia; Fig. 1a), seasonal (winter) incursions of the SWW result in a Mediterranean type climate (Sturman and Tapper, 2006). Summer moisture delivered by easterly winds originating from the Pacific Ocean provides an additional source of precipitation along the southeast Australian coast and Great Dividing Range, resulting in a temperate summer-rain climate. The strength of this moisture advection is influenced by changes in westerly flow at seasonal and interannual timescales (Hendon et al., 2007). The continental island of Tasmania (41–44°S; Fig. 1a) lies in the path of the SWW year-round and is bisected by a northeast–southwest mountain range. Orographic uplift of the SWW over Tasmania results in a hyper-humid west and sub-humid conditions in central and eastern regions as westerly foehn winds strip moisture and negate incursions of easterly moisture (Gentilli, 1972; Sturman and Tapper, 2006; Hill et al., 2009).

The entire eastern coast of mainland Australia and the west coast of Tasmania are climatically suited to the development of rainforest vegetation. A diverse array of vegetation types dominated by *Eucalyptus* species prevails across much of the Australian continent (from the monsoonal tropics to temperate, Mediterranean, and arid regions) and are dependent on varying interactions between climate, soils and fire regime. Fire is a key factor in the vegetation landscape of Australia with, for example, fire being implicated as the only factor capable for explaining the contemporary (restricted) distribution of Australian rainforests (Bowman, 2000). Australia has a well developed Mediterranean flora, particularly in southwest Western Australia, that is characterised by a very diverse array of scleromorphic shrubs that give way to arid zone vegetation as rainfall decreases further.

2.2. Palaeoenvironmental records

2.2.1. Lake-levels

2.2.1.1. Southwest Victoria. Rainfall in southwest Victoria (38°S; Fig. 1a) is delivered almost exclusively by the SWW and is positively correlated with near-surface zonal wind speeds in the modern climate (Fig. 1b). Lake-level reconstructions from closed-basin lakes in southwest Victoria have enabled a reconstruction of effective precipitation spanning the last 10,000 years that proxies westerly derived moisture (Bowler and Hamada, 1971; Harrison and Dodson, 1993; Jones et al., 1998). A marked increase in effective precipitation occurs in the region after 9.5 ka (Fig. 2g), driving high lake-levels that persist until 6 ka (Fig. 2f), after which lake-levels drop substantially. Low and variable values of effective precipitation characterise the period after 3 ka (Fig. 2g), with Lake Keilambete in southwest Victoria displaying a lake-level minimum between 3 and 2 ka, an increase after 2 ka, and a decline since the 18th century (Fig. 2f).

2.2.1.2. Tasmania. The Tasmanian regional lake-level reconstruction published by Harrison and Dodson (1993) is dominated by lakes located in central and eastern Tasmania (41–44°S; Fig. 1a), regions in which rainfall is negatively correlated with westerly wind speed in the modern climate (Fig. 1b; Hendon et al., 2007; Hill et al., 2009). The lake-level synthesis shows a low percentage of lakes full between 14–12 ka and 7–5 ka, a high percentage of lakes full between 11 and 8 ka, and little change since 5 ka (Fig. 2b). Lake Vera is the only lake located in the western hyper-humid zone

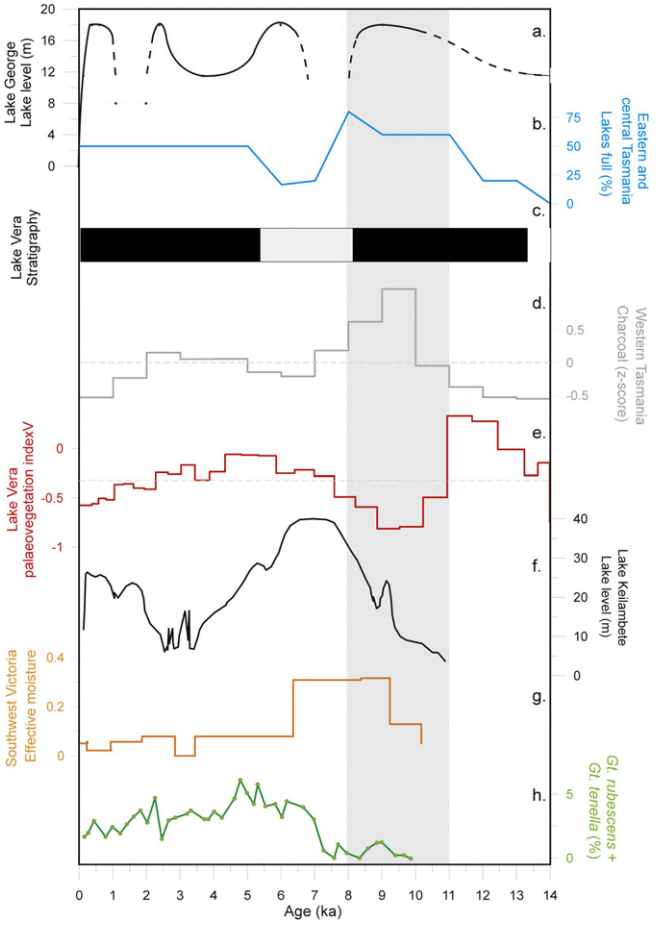

Fig. 2. Palaeoenvironmental data from southern Australia plotted on a calendar year BP timescale: (a) Lake George composite lake-level curve (Site 7, Fig. 1a; De Deckker, 1982; Singh and Geissler, 1985; Fitzsimmons and Barrows, 2010); (b) eastern and central Tasmanian lake-level curve (Site 6, Fig. 1a; Harrison and Dodson, 1993); (c) Lake Vera stratigraphy (Site 5, Fig. 1a; Macphail, 1979); (d) western Tasmanian regional charcoal curve (dashed line indicates the 14 ka mean) (Site 5, Fig. 1a; Fletcher and Thomas, 2010a); (e) Lake Vera palaeovegetation index (Site 5, Fig. 1a; dashed line indicates the 14 ka mean); (f) Lake Keilambete lake-level curve (Site 4, Fig. 1a; Bowler and Hamada, 1971); (g) southwest Victoria effective precipitation curve (Site 4, Fig. 1a; Jones et al., 1998); (h) tropical foraminifera in ocean core MD03-2611 (Site 3, Fig. 1a; Moros et al., 2009). Timescales were developed based on calendar years whenever the original records were published in radiocarbon age scales. Radiocarbon dates were calibrated using Calib 6.1 (Stuiver et al., 2010) and linear interpolations developed between these calibrated dates. See Fig. 1a for the location of sites. Grey shading indicates the early Holocene (11–8 ka) period of weak westerly flow in the Southern Hemisphere.

utilised in Harrison and Dodson's (1993) synthesis. The lithostratigraphy of the Lake Vera record reveals dark-brown clay detritus mud (13–8 ka, black in Fig. 2c) overlain by bluish-grey clay mud deposited between ~8 and 6.5 ka (grey in Fig. 2c), capped in turn by detritus mud after 6.5 ka (black in Fig. 2c) (Macphail, 1979). The change to bluish-grey clay mud between 8 and 6.5 ka implies delivery of terrigenous material into the basin and has two plausible and contrasting explanations: (1) internal reworking of littoral material under a low lake-level stand driven by drier-than-present conditions (Bradbury, 1986); or (2) increased flux of inorganic material in the catchment area resulting from enhanced runoff driven by higher-than-present rainfall.

2.2.1.3. Southeast Australia. Lake George (35°S; Fig. 1b) is a much studied, hydrologically sensitive lake, with a large (800 km^2) flat basin near the southeast Australian coast (Huntington et al., 1908; Cep, 1923; Singh et al., 1981; De Deckker, 1982; Singh and Geissler, 1985; Fitzsimmons and Barrows, 2010). Summer-rainfall in this temperate region is negatively correlated with zonal, near-surface SWW speed in the modern climate (Fig. 1b; Hendon et al., 2007). The fact that historical lake-level fluctuations at Lake George display a good correlation with local rainfall and evaporation demonstrates its sensitivity to monitor past changes in effective precipitation (Jennings, 1981). Optically Stimulated Luminescence (OSL) dating of two outcrops at different elevations above the lake depocentre, in combination with previous palaeoecological studies from the lake, enables a lake-level reconstruction spanning the last 14,000 years (Fig. 2a). Three distinct phases are recognisable based on the OSL geochronology: (1) a permanent $\geq$11.5 m deep lake at 14.2 ± 0.9 ka; (2) aeolian deposition at 9.13 ± 1.2 ka (the pooled mean age of a cluster of statistically identical OSL dates) signifying lake-level lowering from $\geq$15 m deep to below 11.5 m prior to this time; (3) a fluctuating lake between 6.0 ± 0.4 and 0.34 ± 0.03 ka, with a clear low stand at 3.7 ± 1.0 ka (~11.5 m), a high-stand between 2.4 ± 0.2 ka ($\geq$15 m) and aeolian deposition at 1.1 ± 0.2 ka (<11.5 m) (Fitzsimmons and Barrows, 2010). Palaeoecological analyses from Lake George are in broad agreement with the OSL-based chronology of lake-level fluctuations (Fig. 2a), suggesting the presence of a permanent lake and forest development between 12.2 and 8.5 ka, ephemeral lake conditions between 8.5 and 3.2 ka, and a predominantly dry lake-bed thereafter (Singh et al., 1981; De Deckker, 1982).

2.2.2. Tasmanian vegetation and fire

Several pollen and charcoal profiles from the hyper-humid west of Tasmania reveal regionally synchronous changes in climate-sensitive plant taxa over the post-LGM period (Macphail, 1979; Markgraf et al., 1986; Fletcher and Thomas, 2010a). Lake Vera (42°S) lies within *Nothofagus* and Podocarpaceae-dominated rainforest in western Tasmania (Macphail, 1979), a region solely dependent on the SWW for precipitation that displays a strong positive correlation between westerly wind speed and precipitation in the modern climate (Fig. 1b; Hendon et al., 2007; Hill et al., 2009). A log-normalized ratio of *Nothofagus-Atherosperma*/*Phyllocladus* (Podocarpaceae) was calculated, based on the Lake Vera pollen record published by Macphail (1979). The rationale behind the index is the varying climatic envelopes of the modern species' ranges utilised in the index: *Nothofagus cunninghamii* and *Atherosperma moschatum* grow in drier regions than *Phyllocladus asplenifolius*, which is presently restricted to the cool-wet temperate rainforests of Tasmania (Read and Busby, 1990). The index tracks compositional change in the rainforests around Lake Vera in response to changes in relative moisture delivered by the SWW in this region and is, thus, a proxy for SWW influence. Increasing relative moisture is evident in the Lake Vera palaeovegetation index between 14–11.7 ka and 9.5–6 ka, and a decreasing relative moisture is observed between 11.7–9.5 ka and 4.5 ka to the present (Fig. 2e).

Fire regimes, as inferred from the charcoal content in sediment cores, are driven by climatic change over multi-millennial timescales (Power et al., 2008) and are an effective proxy of negative moisture anomalies in hyper-humid regions, considering that fuel is not a limiting factor for fire occurrence in the cool temperate southern latitudes (Whitlock et al., 2007; Moreno et al., 2010). A charcoal curve for western Tasmania (Fletcher and Thomas, 2010a; Fletcher and Moreno, 2011) displays clear multi-millennial trends that reflect regional trends in moisture-driven fire regime: (1) below average charcoal between 14 and 12 ka; (2) increasing charcoal from 12 ka, peaking between 10 and 9 ka; (3) charcoal decreases from 9 ka and reaches a minimum between 7 and 5 ka; (4) charcoal increases from 5 to 2 ka, and then (5) a decline since 2 ka.

2.2.3. The Leeuwin Current

The Leeuwin Current is a warm water surface current that advects tropical waters of the Indo-Pacific Warm Pool poleward along the west coast of Australia (Fig. 1a; Weaver and Middleton, 1989). The SWW have a significant effect on the strength, speed, and eastward propagation of the Leeuwin current (Middleton and Bye, 2007) along the annual cycle with weakest/slowest flow during summer concurrent with a poleward displacement of the SWW; and strongest/fastest flow during winter, when the equatorward displacement of the SWW results in a more westerly aspect to wind direction that promotes advection of warm surface water along the south Australian coast (Middleton and Bye, 2007). The composition of foraminifera in ocean core MD03-2611 (36°S), located in cool waters off the southern Australian coast toward the eastern limits of the present-day Leeuwin Current (Fig. 1a), proxies the strength and eastward penetration of the Leeuwin Current (Moros et al., 2009). Tropical foraminifera, *Globoturborotalita rubescens* and *Globoturborotalita tenella*, non-indigenous to the cold Southern Ocean waters and transported to the site by the Leeuwin Current, are virtually absent between 10 and 7.5 ka, signalling a failure of the Leeuwin Current to penetrate eastward to the site (Fig. 2h). Percentage values for *G. rubescens* and *G. tenella* increase steadily between 7.5 and 6 ka and peak between ca. 5.5 and 5 ka, after which these taxa decline in importance to the present. The steady increase in tropical foraminifera reflects penetration of the Leeuwin Current warm surface water to the site and suggests a stronger-than-present Leeuwin Current between 5.5 and 5 ka that is followed by a multi-millennial decrease to present conditions.

2.2.4. Summary

The multi-proxy evidence presented here for southern Australia and Tasmania highlights a common multi-millennial pattern in moisture regime and ocean circulation changes since 14 ka that mirrors the relationship between SWW speed and precipitation in the modern climate (Fig. 1b). The period between 14 and 5 ka is marked by strikingly synchronous trends across the region, with distinct phases occurring between 14–12, 11–8, and 7–5 ka. A degree of regional heterogeneity and asynchrony develops in the records after 5 ka.

The interval between 14 and 12 ka reflects a period of high relative moisture and low fire incidence in western Tasmania (Fig. 2) and southwest Victoria (Turney et al., 2006b). Together with low lake-levels in eastern Tasmania and Lake George in southeast Australia, the data suggest strong SWW flow over the region. Low relative moisture and high charcoal contents prevailing in western Tasmania between 11 and 8 ka were concurrent with high lake-levels in eastern Tasmania and at Lake George, mirroring the effects

of decreased westerly flow over these regions in the modern climate (Fig. 1b) and indicating a multi-millennial phase of attenuated SWW flow at this time. The period between 7 and 5 ka is marked by a reversal of the previous trend with a multi-millennial phase of enhanced westerly flow that led to a moisture increase in western Tasmania and southwest Victoria, along with low lake-levels in eastern/central Tasmania between 8 and 6 ka and south-east Australia (Lake George) between ~9 and 6 ka. This was concurrent with a decrease in palaeofire in western Tasmania and deposition of terrigenous material in Lake Vera resulting from enhanced runoff driven by a multi-millennial increase in westerly flow across the entire region. A 'westerly maximum' is apparent at ~6 ka and is supported by a sharp increase in tropical foraminifera delivered by the Leeuwin Current from negligible values at 7.5 ka to a greater-than-present maximum between 5.5 and 5 ka in deep sea core MD03-2611 (Fig. 2h).

A multi-millennial decrease in moisture and increase in charcoal in western Tasmania from 5 to 2 ka is consistent with a cessation of terrigenous input into Lake Vera and lake-level lowering at Lake Keilambete in southwest Victoria, reflecting a decrease in westerly precipitation. After 2 ka, western Tasmanian charcoal declines substantially, counter to the continued drying trend indicated by the Lake Vera palaeovegetation index, yet consistent with a return to a high lake-level at Lake Keilambete. A gradual multi-millennial decrease in tropical foraminifera in ocean core MD03-2611 is consistent with the Lake Vera index, suggesting a multi-millennial decrease in SWW flow toward the present. Lake-levels in eastern and central Tasmania remain invariant from 5 ka onward, while Lake George undergoes a moderate lowering of lake-level centred at 3.7 ± 1 ka. This event is not replicated in other southern Australian sites, although the large error associated with the timing of this event precludes confident correlations with other records. The drop in Lake George lake-level between ca. 2.5 and 0.5 ka is concomitant with high a lake-level at Lake Keilambete, suggesting a return to east-west anti-phasing prevalent under increased SWW flow.

3. New Zealand

3.1. Present environment

New Zealand is a long narrow series of islands located between 34 and 45°S, predominantly within the SWW zone of influence (Fig. 1a). North Island extends into the sub-tropical high pressure zone and receives moisture from the warm northern oceans (Pacific Ocean), resulting in a warm temperate climate (Sturman and Tapper, 2006). South Island is subject to cooler temperatures and is under the permanent influence of the SWW (McGlone et al., 1993; Sturman and Tapper, 2006). The northwest–southeast trending Southern Alps bisect the South Island into distinct west and east climate zones: a hyper-humid west and a humid to sub-humid east (McGlone et al., 1993). Precipitation is significantly correlated to westerly wind speed, with an increase (decrease) in westerly flow resulting in a steepening (relaxing) of the west–east precipitation gradient (McGlone et al., 1993). Southerly winds deliver precipitation to the south of the South Island, with the orographic rain-shadow zone restricted to the central east (Otago) region (McGlone et al., 1993). The Southern Alps are glaciated, with glacial dynamics governed by both temperature (Anderson and Mackintosh, 2006) and westerly derived precipitation (Fitzharris et al., 1992).

The complex topography and geology of New Zealand produces a wide variety of microclimatic zones that host a complex and highly endemic flora. Broadly speaking, the principal vegetation units are forest and grassland that are primarily determined by temperature, moisture and disturbance (Dodson, 1998). Taxonomically diverse hardwood trees dominate the forests of the warm temperate North Island and were much more widespread before the arrival of humans (~0.8 ka) (Wardle, 1991; McGlone et al., 1993; Wilmshurst et al., 2008). In the South Island, *Nothofagus* and podocarp forests dominate the high-rainfall west and southern regions up to the tree-line, where stunted woody taxa and herbaceous plants prevail in the oceanic climate (Wardle, 1991). Grasslands prevail in the sub-humid central eastern region, owing their present spatial extent to the combined effects of dry westerly foehn winds and anthropogenic disturbance (e.g. McGlone and Moar, 1998; McWethy et al., 2009).

3.2. Palaeoenvironmental records

3.2.1. West coast South Island vegetation

The Okarito Bog pollen record (Newnham et al., 2007) from the west coast of South Island (43°S; Fig. 1a) is located within the westerly derived high-rainfall zone, a region that displays a strong positive correlation between zonal westerly wind speed and precipitation (Fig. 1b; McGlone et al., 1993; Ummenhofer and England, 2007). Unfortunately, no dating was performed on the Holocene portion of this record. A linear extrapolation is used from the uppermost date (10.9 ka) to the present, although this is likely inappropriate given the sedimentary changes through this section (Newnham et al., 2007). Nevertheless, trends in aquatic taxa in the Okarito Bog pollen record show a dynamic response to moisture changes over the last 14,000 years (Fig. 3c). The transition from an LGM lake to a post-glacial bog was punctuated by the following multi-millennial fluctuations in aquatic pollen content: high aquatic pollen content between 14 and 11.5 ka; a significant reduction in aquatic pollen content between 11.5 and 8 ka; increasing aquatic pollen between 7.5 and 5 ka; and a multi-millennial decrease to present (Fig. 3c).

3.2.2. East South Island precipitation

Prebble and Shulmeister (2002) conducted a quantitative reconstruction of effective precipitation based on phytolyths in Otago (45°S; Fig. 1a), a region affected by dry foehn winds that displays a negative correlation between zonal flow and precipitation in the modern climate (Fig. 1b). The stratigraphy of the site is complex, and the chronology relies on three radiocarbon dates and five OSL dates that have substantial error ranges, precluding the development of a precise age model. Prebble and Shulmeister (2002) report an increase in effective precipitation beginning at

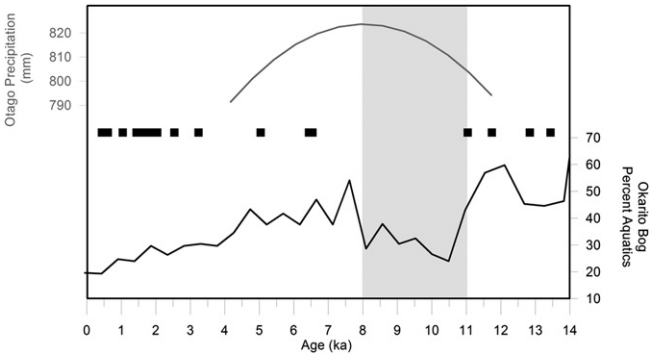

Fig. 3. Palaeoenvironmental data from New Zealand plotted on a calendar age scale: (a) Otago precipitation curve (Site 9, Fig. 1a; Prebble and Shulmeister, 2002); (b) Southern Alps glaciations (Lowell et al., 1995; Shulmeister et al., 2004; Schaefer et al., 2009); (c) Okarito Bog aquatic pollen content (Site 8, Fig. 1a; Newnham et al., 2007). See Fig. 1a for the location of sites. Grey shading indicates the early Holocene (11–8 ka) period of weak westerly flow in the Southern Hemisphere.

12 ka, peaking at ~8.5 ka and decreasing toward 4 ka (Fig. 3a). Depositional hiatuses effectively terminate the record at ~4 ka.

3.2.3. Southern Alps glacier dynamics

The temperate glaciers of New Zealand are sensitive to climate change, although there is some debate over what component of climate exerts the greatest influence over changes in glacier mass balance in the region, with both temperature and precipitation purported as the dominant control (Fitzharris et al., 1992; Anderson and Mackintosh, 2006; Purdie et al., 2011). A significant relationship between the strength of SWW flow and glacial mass balance was observed by Fitzharris et al. (1992) and it is clear that westerly derived precipitation is an important factor in glacial dynamics in this region. A substantial body of work has been devoted to establishing a chronology of glacial fluctuations in the Southern Alps that reveals multi-millennial trends that most likely reflect both precipitation and temperature effects (e.g. Gellatly et al., 1988; Denton and Hendy, 1994; Fitzsimons, 1997; Barrows et al., 2007; McCarthy et al., 2008; Schaefer et al., 2009). A salient feature of the glacial record (Fig. 3b) is a deep glacial recession between ~11 and 7 ka, which Shulmeister et al. (2004) argue reflects weak westerly flow across the region effectively starving glaciers of moisture. Increased westerly flow and/or lower temperatures are sufficient to account for widespread and well advanced glaciation between 14 and 11 ka and for neoglaciation since 7 ka (Moreno et al., 2009; Rojas and Moreno, 2010; Shulmeister et al., 2010).

3.2.4. Summary

Clear multi-millennial trends are evident in the palaeoenvironmental data from New Zealand's South Island: 14–11, 11–8, 7.5–4.5, and 4.5–0 ka. The period between 14 and 11 ka is characterised by relatively high aquatic pollen content at Okarito Bog and glacial advances in the Southern Alps, likely reflecting a combination of cool temperatures and strong westerly flow over the region. Between 11 and 8 ka, aquatic pollen content declines substantially at Okarito Bog on the west coast and precipitation increases in Otago to a maximum at ~8.5 ka. Anti-phasing of west and east precipitation anomalies is consistent with the modern relationship between South Island rainfall and westerly wind speed and the lack of (or very much limited) glacial advance at this time is contemporaneous with weak westerly flow. A combination of maximum Holocene aquatic pollen content at Okarito Bog and decreasing precipitation east of the Southern Alps in Otago, contemporaneous with renewed glaciation, suggests an increase in westerly flow over the South Island between 7.5 and 4.5 ka. After 4.5 ka, aquatic pollen content in the Okarito record shows a gradual decline toward the present; suggesting a possible decline in westerly flow over the region, while, in contrast, the spread of the podocarpaceous tree *Dacrydium cupressinum* recorded across Southland and Otago (South Island New Zealand) has been interpreted as indicating an increase in westerly flow across the region after ca. 3 ka (McGlone et al., 1993).

4. Southern South America

4.1. Present environment

South America stretches from north of the equator to 55°S, transgressing a broad range of climatic zones, from warm equatorial to cold sub-Antarctic. In the zone of westerly influence, large amounts of year-round rainfall inundate areas west of the Andes south of ~38°S, while in the rain-shadow east of the Andes, sub-humid to semi-arid conditions result from persistent foehn winds. Abundant precipitation of westerly origin sustains temperate rainforests on the Pacific side of the Patagonian Andes (the region south of 40°S in South America). Climatic segregation of the vegetation has led to the recognition of Valdivian, North Patagonian, and sub-Antarctic rainforest communities in Patagonia along a gradient of increasing precipitation and wind speeds, lower temperatures and length of the growing season. Vegetation east of the Andes is dominated by the sub-humid to semi-arid Patagonian Steppe to the east as moisture decreases. Seasonal forcing drives the SWW north (south) in winter (summer) relative to their core region of strongest wind speeds (~50°S), resulting in a winter (summer) dominant rainfall climate north (south) of ~50°S.

4.2. Palaeoenvironmental records

4.2.1. Lake-levels

4.2.1.1. West of the Andes – central Chile. Laguna Aculeo is located in the Mediterranean climate zone of central Chile toward the northern limits of the zone of westerly influence (33°S; Fig. 1a), an area in which local precipitation is positively correlated with westerly wind speed (Fig. 1). The hydrologic balance of this relatively closed-basin lake is dependent on the westerlies for recharge (Jenny et al., 2003). A precipitation curve spanning the last 10,000 years has been derived from changes in the lake-level of Laguna Aculeo through this time that is characterised by the following sequence (Fig. 4f; Jenny et al., 2003): low effective precipitation between 10 and 8.6 ka; a slight increase in precipitation at 8.6 ka; a marked increase at 5.6 ka that persists until 3 ka; after which a variable and slightly increasing precipitation regime prevails until the present.

Abarzúa et al. (2004) present stratigraphic evidence from Lago Tahui (~43°S), a small closed-basin lake located in an intermorainal depression in east-central Isla Grande de Chiloé, NW Patagonia, a region in which precipitation is strongly correlated with westerly wind speed. The record includes piston cores obtained along a bathymetric transect, correlated on the basis of tephra layers and radiocarbon dates. Cores collected from the shallow portion of the lake revealed a basal silty gyttja overlain by woody gyttja (with >5 cm diameter tree trunks and branches), overlain in turn by coarse organic detritus gyttja, and gyttja until the present. The authors interpreted these data as evidence for a regressive lake phase that led to the centripetal expansion of a swamp forest environment at intermediate depths in the lake, followed by a transgressive phase and persistence of the lake until today (Abarzúa et al., 2004). The available chronology indicates that lake-levels in Lago Tahui remained stationary below the modern elevation between 11.5 and 7.8 ka, implying a decline in regional precipitation delivered by the SWW during that time (Abarzúa et al., 2004).

4.2.1.2. East of the Andes – Argentine Patagonia. Lago Cardiel is a deep and much studied closed-basin lake located within the dry Patagonian Steppe of Argentina (49°S; Fig. 1a), a region receiving as little as 150 mm of annual rainfall (Markgraf et al., 2003; Gilli et al., 2005a; Ariztegui et al., 2009). The site lies in the rain-shadow east of the Andes Cordillera close to the present-day zone of maximum SWW speeds (50°S), and displays a negative correlation between zonal wind strength and local precipitation that results from significant evaporative moisture loss as dry foehn winds strip moisture from the region under strong westerly flow (Fig. 1b; Garreaud, 2007). A recent lake-level reconstruction from Lago Cardiel reveals substantial lake-level changes since 14 ka that reflect changes in precipitation and evaporation (Ariztegui et al., 2009) (Fig. 4a). The lake was low between 14 and 12.3 ka, and was followed by an abrupt transgressive phase that led to higher-than-modern lake-levels between ~11–8 ka, representing a ~100 m increase in lake-level and reflecting a significant change

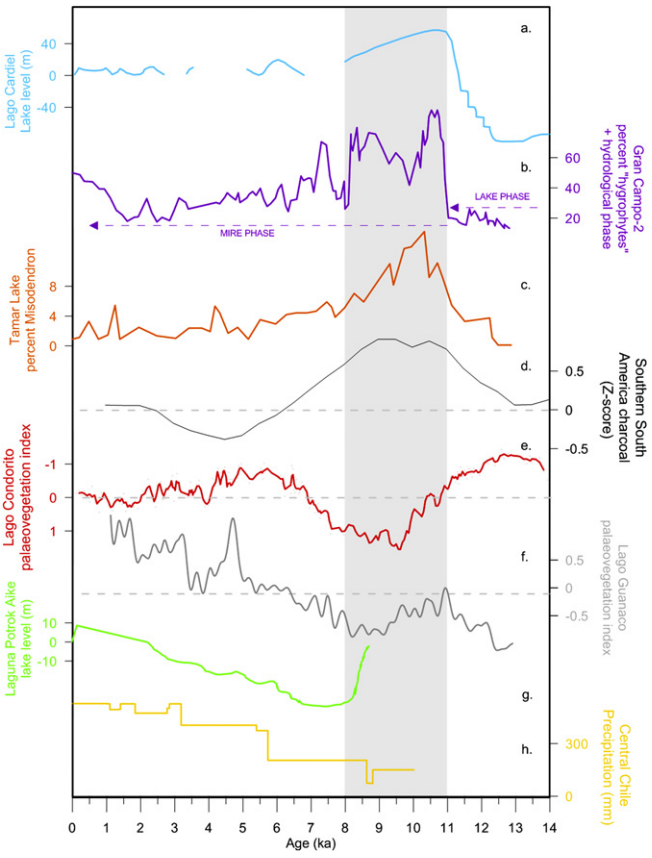

Fig. 4. Palaeoenvironmental data from southern South America plotted on a calendar age scale: (a) Lago Cardiel lake-level reconstruction (dashed line indicates the modern lake-level) (Site 12, Fig. 1a; Ariztegui et al., 2009); (b) Gran Campo-2 hygrophyte curve and hydrological phase (Site 14, Fig. 1a; Fesq-Martin et al., 2004); (c) Lago Tamar *Misodendron* curve (Site 15, Fig. 1a; Lamy et al., 2010); (d) southern South American charcoal curve (dashed line indicates the 14 ka mean) (Power et al., 2008); (e) Lago Condorito palaeovegetation index (dashed line indicates the 14 ka mean) (Site 11, Fig. 1a; Moreno, 2004); (f) Lago Guanaco palaeovegetation index (dashed line indicates the 12 ka mean) (Site 13, Fig. 1a; Moreno et al., 2010); (g) Laguna Potrok Aike lake-level reconstruction (Site 16, Fig. 1a; Anselmetti et al., 2009); (h) Laguna Aculeo precipitation reconstruction (Site 10, Fig. 1a; Jenny et al., 2003). See Fig. 1a for the location of sites. Grey shading indicates the early Holocene (11–8 ka) period of weak westerly flow in the Southern Hemisphere.

in the delivery of atmospheric moisture into the extra-Andean region of Central Patagonia. After 8 ka, lake-levels fell, fluctuating repeatedly between +15 m and the present-day level (Markgraf et al., 2003; Ariztegui et al., 2009).

Another much studied lake basin in Argentine Patagonia, Laguna Potrok Aike (52°S; Fig. 1a), lies south of the modern core of the SWW in a region where modern precipitation displays no statistically significant relationship with SWW speed (Fig. 1b). A possible reason for the lack of correlation of precipitation at this site with SWW speed is the proximity of both the Andes and the Atlantic Ocean, providing precipitation spilling eastward with the westerly winds and increased humidity from the South Atlantic under weak westerly flow, respectively. A lake-level reconstruction from Potrok Aike (Anselmetti et al., 2009) reveals a lake regressive phase from >8.5 ka to a lake-level minimum at ~7 ka, after which a multi-millennial lake-level transgression started and has persisted until the present (Fig. 4e).

4.2.2. Western Patagonian vegetation

4.2.2.1. North of ~50°S. A consensus exists between virtually all vegetation-based multi-millennial moisture reconstructions from within the westerly zone of influence north of ~50°S in western Patagonia (e.g. Villagran, 1988; Jenny et al., 2002; Abarzúa et al., 2004; Haberle and Bennett, 2004; Moreno, 2004; Latorre et al., 2007; Markgraf et al., 2007; Abarzúa and Moreno, 2008). The well dated (18 AMS radiocarbon dates) pollen record from Lago Condorito (41°S; Fig. 1a) can be used to represent changes in SWW-derived moisture in this region over the last 14,000 years. Lago Condorito is a small closed-basin lake, located in the transitional zone between the warm and seasonal Valdivian rainforests and the cool, perennially wet North Patagonian rainforests (Moreno, 2004). A pollen-based normalized *Eucryphia* + *Caldcluvia* (Valdivian taxa)/Podocarpaceae (North Patagonian taxa) index calculated for this site proxies intensity variations and movements in the northern edge of the westerlies and reveals clear multi-millennial trends in moisture balance (Fig. 4e; Moreno, 2004). Initially, above average moisture between ~14 and 12.5 ka is evident, followed by a declining moisture trend with negative anomalies between ~10.5 and 7.8 ka and characterised by strongly negative values between 9.5 and 8.5 ka, revealing a decrease in westerly derived moisture north of the modern zone of strongest westerly flow during this time (Fig. 4e). The index suggests that moisture increased until a maximum at 6–5 ka, reflecting an increase in westerly derived precipitation north of the core of the westerlies, after which a multi-millennial decrease is evident (Fig. 4e).

4.2.2.2. South of ~50°S. Recent palaeovegetation-based interpretations of westerly derived moisture variations since 14 ka from south of 50°S in western Patagonia are divided between two opposing models of westerly change (Lamy et al., 2010; Moreno et al., 2010; Fletcher and Moreno, 2011). Important for both models is the interpretation of a normalized *Nothofagus*/Poaceae pollen index (NPI) from Lago Guanaco, a small closed-basin lake situated near the modern forest-steppe ecotone (52°S; Moreno et al., 2010) in an area where local precipitation is strongly and positively correlated with zonal wind speed (Fig. 1b). The NPI from Lago Guanaco was interpreted by Moreno et al. (2010) as a local sensor of past shifts of the forest-steppe ecotone and the amount of SWW-derived precipitation spilling eastward over the Andes. The Lago Guanaco index displays increasing woody vegetation/moisture at the site between 13 and 11 ka, steppe/decreasing moisture between 11 and 8 ka and an increasing, albeit variable, forest expansion/moisture increasing trend thereafter (Fig. 4f). In a subsequent study, Lamy et al. (2010) offer an alternative interpretation of the NPI, with negative/steppe (positive/forest) excursions considered as evidence for increased (decreased) evaporation at the site under enhanced (attenuated) westerly flow.

The location of the forest-steppe ecotone in Patagonia is dependent on moisture balance (Paruelo et al., 1998) and is influenced by the amount and seasonality of westerly precipitation spilling eastward over the Andes and the amount of evaporation resulting from desiccating (westerly) foehn winds. Lago Guanaco presently lies within steppe vegetation, despite an average annual rainfall (720 mm p/a; Moy et al., 2008) above the suggested threshold for steppe development in Southern Patagonia and Tierra del Fuego (500–350 mm p/a; Tuhkanen, 1992; Tuhkanen et al., 1992), which Lamy et al. (2010) interpret as a reflection of the dominant influence of evaporation (strongest in the summer high wind period) over the local moisture regime and vegetation type. They consider trends toward steppe (forest) in the index to be driven by stronger (weaker) westerly flow and increased (decreased) evaporation. An important factor neglected by those authors is that the modern forest-steppe ecotone in Southern Patagonia is not in equilibrium with climate, but is the result of European deforestation (Veblen and Markgraf, 1988; Huber and Markgraf, 2003). Forest covered the landscape more than more

than ~25 km *east* of Lago Guanaco prior to AD 1881 (Dixie, 1881), implying that evaporation does not limit forest development in the vicinity of Lago Guanaco today, and that precipitation exerts the dominant control over vegetation in that area. Despite this, it is possible that, given the location of the site east of the orographic divide, under varying westerly wind regimes, the tension zone between evaporation and precipitation dominance over vegetation shifts east or west of its present location to the east of Lago Guanaco.

Sediments retrieved from the Gran Campo-2 site (52°48′37″S, 73°55′46′W; Fesq-Martin et al., 2004), a minerotropic mire located west of the Andes orographic divide where the relationship between precipitation and westerly wind strength is positive (Fig. 1b), show a transition from a lake to a mire at that site (between 11.2 and 10.9 ka), in concert with an abrupt and sustained increase in "hygrophyte" pollen taxa between 11 and 8 ka (Fig. 4b) that reflects the colonisation of a former lake by the principal mire forming plant, *Marsippospermum* spp., and peatland dynamics thereafter (Fesq-Martin et al., 2004), a process known as terrestrialisation, when lakes infill under stable or dropping lake-levels (Futyma and Miller, 1986; Korhola, 1995; Brugam and McCance Johnson, 1997; Weckstrom et al., 2010), implying a transition to drier climate between 11.2 and 10.9 ka. After ~8.5 ka, an increase in moisture is reflected by the establishment of Magellanic Moorland taxa (*Astelia pumila* and *Donatia fascicularis*) at the site (Fesq-Martin et al., 2004).

A partially published pollen record from Lago Tamar (52°54.21′S, 73°48.07′W; Lamy et al., 2010), located west of the Andes, shows a marked and sustained increase in *Misodendron* pollen, a hemiparasite on *Nothofagus* trees, between 11.5 and 8.5 ka (Fig. 4c; Lamy et al., 2010). The *Misodendron* peak is temporally synchronous with the negative moisture anomalies identified at Lago Guanaco and Lago Condorito (Fig. 4e, f). Studies of modern pollen dispersal in Southern Patagonia reveal greatest *Misodendron* pollen content at the relatively dry and open forest-steppe ecotone (Markgraf et al., 1981; Paez et al., 2001). Numerical analysis of modern pollen data from the region reveals that *Misodendron* pollen content is positively correlated with *Nothofagus* and other forest indicators (Dale et al., 2010). Thus, while interpretation of the *Misodendron* curve is complicated by these factors, it is likely to reflect a trend toward canopy openness, which is consistent with a trend toward drier conditions.

4.2.3. Western Patagonia fire

Peak charcoal activity is evident between 12.5 and 9.5 ka in sites located between 40 and 55°S, where rainfall is positively correlated with zonal wind speed (Heusser, 2003; Haberle and Bennett, 2004; Huber et al., 2004; Moreno, 2004; Whitlock et al., 2007; Abarzúa and Moreno, 2008; Massaferro et al., 2009; Markgraf and Huber, 2010). The regional charcoal curve for SSA (Power et al., 2008) captures this trend remarkably well (Fig. 4d) and displays a clear correlation to the palaeovegetation indices from Lago Guanaco and Lago Condorito (Fig. 4e, f). The charcoal data indicate increasing charcoal from 12.5 to 9.5 ka; decreasing charcoal from 9.5 to 3.5 ka; increasing charcoal to 2.5 ka; and little change thereafter (Fig. 4b).

4.2.4. Summary

High relative moisture in the northwest Patagonian palaeovegetation index and low southern South American charcoal values between 14 and 12 ka imply strong westerly flow that is consistent with dry conditions and low lake-levels east of the Andes Cordillera at Lago Cardiel. The available evidence indicates a multi-millennial decrease (increase) in moisture (fire) in northwest Patagonia from ~12.5 ka. In southwest Patagonia, increased moisture in Lago Guanaco, cool-wet conditions in Gran Campo-2 (Fesq-Martin et al., 2004) and moist conditions at Isla de los Estados (54°50S; 64°40W; Ponce et al., 2011) indicates an asymmetry of moisture changes north and south of the modern westerly core that implies a southward shift of the SWW at this time. After 11 ka, negative moisture trends at Lago Condorito and L. Guanaco, warmer and drier conditions at Isla de los Estados (Ponce et al., 2011) and terrestrialisation of the Gran Campo-2 site indicate a decrease in SWW-derived moisture that persists until ~8 ka, revealing negative moisture trends across the entire zone of westerly influence, coeval with peak fire activity in high-rainfall regions throughout Patagonia. East of the Andes, above modern lake-level at Lago Cardiel between ~11 and 8 ka (Fig. 4a) and a trend toward increased relative moisture across sites in Argentina (Mancini et al., 2008) are consistent with decreased SWW influence, revealing synchronous and co-variable changes in westerly wind behaviour north and south of the core of the SWW (ranging between 41 and 52°S) that led to decreased moisture west of the Andes and less intense foehn winds and increased incursions of Atlantic Ocean moisture to the east.

Increasing relative moisture in the west and a concomitant decrease in southern South American charcoal is evident after ~8 ka toward an apparent 'moisture maximum' in northwest Patagonia between 6 and 5 ka. This pattern is consistent with increasing moisture in southwest Patagonia (Fig. 4e, f) and decreased lake-levels at Lago Cardiel (Fig. 4a). Moreover, these trends are consistent with a stepwise increase in effective precipitation in central Chile at 8.6 ka and 5.6 ka (Fig. 4f) and a trend toward drier climate conditions in Argentina, east of the Andes Cordillera (Mancini et al., 2008). These regionally consistent trends imply that the westerlies increased in strength across their entire zone of influence. Moisture indices diverge after 5 ka, with a slight multi-millennial decrease in relative moisture evident in northwest Patagonia (Fig. 4e), and multi-millennial moisture increases in southwest Patagonia and central Chile (Fig. 4f, h). Interestingly, a lake-level regression starting >8.7 ka at Laguna Potrok Aike (Fig. 4g), east of the Andes in a zone of zero statistical correlation between westerly wind speed and precipitation (Fig. 1b), followed by a transgression ~7 ka occurs in concert with the Lago Guanaco palaeovegetation (moisture) index located at the same latitude (52°S), suggesting that multi-millennial scale changes in moisture at Laguna Potrok Aike have varied with similar timing and direction as records from areas positively correlated with westerly wind strength during the Holocene. Charcoal values increase after 3.5 ka and remain stable, as does the level of Lago Cardiel (Fig. 4a, d). The effective precipitation curve from Laguna Aculeo shows further increases at 3.2 ka and 2 ka, reflecting an increase in westerly derived moisture in that region (Fig. 4h).

5. Southern Africa

5.1. Present environment

The climate of southern Africa is dominated by the sub-tropical high pressure system resulting from descending Hadley Cell air and the region is generally dry (Tyson and Preston-Whyte, 2000). Seasonal intrusions of monsoonal rain are important during summer in the north of the region. The SWW exert a direct influence on the climate of the southwest tip (the Western Cape), imparting a winter wet Mediterranean climate in that region, while the Eastern Cape is reliant on easterly sourced precipitation delivered during the summer months when westerly flow is weak and the trade winds are displaced southward (Tyson and Preston-Whyte, 2000). This easterly precipitation source is bolstered by the warm southward bound Agulhas Current that flows along the east African coast, resulting in frequent mists (Eeley et al., 1999). The dominance of the trade winds and the cold north-flowing Benguela Current (driven in

part by the SWW) result in a hyper-arid desert on the western coast of southern Africa (Namibia) that grades to the Mediterranean climate zone of the Western Cape further south as the SWW become important (Tyson and Preston-Whyte, 2000).

Southern Africa hosts one of the most diverse vegetation types on Earth, the Fynbos (Mucina and Rutherford, 2006). The Fynbos is comprised of a startlingly diverse array of shrubs that grow on the nutrient-poor geologies of the Western Cape Mediterranean climate zone (Mucina and Rutherford, 2006). To the north and centre of southern Africa, aridity prevails and desert-adapted flora predominate that grade in to savannah biomes as the monsoonal influence increases. The higher relative moisture in the southeast gives rise to a slightly more woody vegetation that transitions into the grasslands and savannah of the northern interior and humid forest patches in relatively moist areas on the east coast (Eeley et al., 1999; Mucina and Rutherford, 2006).

5.2. Palaeoenvironmental records

5.2.1. Western Cape organic sediment accumulation

The dry environment of southern Africa is preclusive to organic sediment accumulation, a facet that would have been amplified (weakened) under past climate regimes in which drier (wetter) conditions prevailed. Preserved organic beds spanning the late Pleistocene to the present are rare in the Western Cape (32–34°S; Fig. 1a), a region wholly dependent on the SWW for precipitation that displays a positive correlation between westerly wind speed and precipitation in the modern climate (Fig. 1b). Fig. 5b shows a plot of the number published organic profiles from the Western Cape region at 1000-year time steps (based on the studies of Schalke, 1973; Meadows, 1988; Meadows and Sugden, 1991; Street-Perrott and Perrott, 1993; Meadows et al., 1996; Meadows and Baxter, 2001). A very low number of profiles date to the period between 14 and 9 ka. While this trend may reflect non-climatic factors, such as a lack of discovery and/or publication of records, the long history of palaeoclimatic research in this region suggests that the lack of organic profiles between 14 and 9 ka may reflect aridity through all or the latter part of this time-span. After 9 ka, the number of published organic sequences increases two-fold and remains high until the present, possibly reflecting more humid conditions since 9 ka.

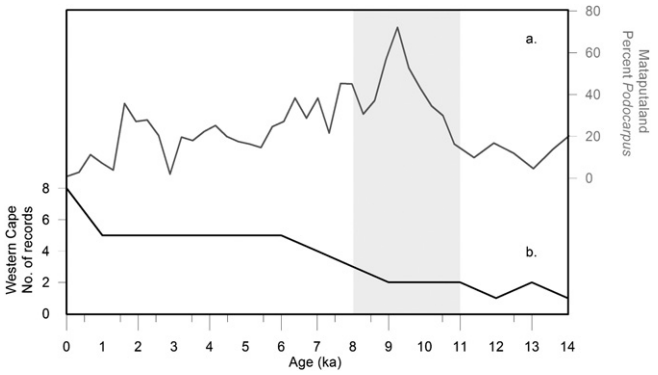

Fig. 5. Palaeoenvironmental data from southern Africa plotted on a calendar age scale: (a) Matputaland pollen record *Podocarpus* values (Site 2, Fig. 1a; Finch and Hill, 2008); (b) Western Cape organic accumulation (Site 1, Fig. 1a; Schalke, 1973; Meadows, 1988; Meadows and Sugden, 1991; Street-Perrott and Perrott, 1993; Meadows et al., 1996; Meadows and Baxter, 2001). Timescales were developed based on calendar years whenever the original records were published in radiocarbon age scales. Radiocarbon dates were calibrated using Calib 6.1 (Stuiver et al., 2010) and linear interpolations developed between these calibrated dates. See Fig. 1a for the location of sites. Grey shading indicates the early Holocene (11–8 ka) period of weak westerly flow in the Southern Hemisphere.

5.2.2. Coastal southeast Africa – Matputaland vegetation

A pollen record from Matputaland in coastal southeast Africa (28°S; Fig. 1a), within the zone of negative correlation between westerly wind speed and precipitation (Fig. 1b) and a region dependent on easterly incursions of moisture from the Indian Ocean, tracks moisture-driven vegetation changes through the late Quaternary (Finch and Hill, 2008). Finch and Hill (2008) reconstructed relative moisture changes at their Matputaland site based predominantly on changes in *Podocarpus* pollen, a humid forest tree (Eeley et al., 1999) that is absent from the site today (Finch and Hill, 2008). Based on this premise they inferred relatively dry conditions and low *Podocarpus* pollen values (<15%) between 14 and 11 ka, followed by a sharp increase in moisture and the establishment of *Podocarpus* forest at the site (pollen values >70%) between 11 and 9.2 ka, after which a steady decline in values between 9.2 and 5.4 ka indicates a decline in available moisture and a reduction of this forest type (Fig. 5a). After 5.4 ka, decreasing and variable *Podocarpus* values possibly indicate a variable climate trending toward drier conditions (Fig. 5a).

5.2.3. Summary

The pattern of multi-millennial changes in moisture regimes in southern South Africa is consistent with the modern relationship between westerly flow and precipitation. Little information is present for conditions in the Western Cape region between 14 and 11 ka, although a review of palaeoenvironmental data from this region depicts the LGM and late Pleistocene as cool and wet (Meadows and Baxter, 1999). Dry conditions (low *Podocarpus* values) on the southeast coast at this time are consistent with the modern relationship between zonal wind strength and precipitation under increased westerly flow and the evidence suggests a strengthening of westerly flow across southern South Africa between 14 and 11 ka. A sharp increase in *Podocarpus* pollen and the establishment of humid forest on the southeast coast between ~11 and 8 ka is consistent with decreased westerly flow and a concomitant increase in incursions of easterly moisture sources and coastal mists. The Western Cape is represented by very few organic sequences between 11 and 9 ka, with the review of Meadows and Baxter (1999) suggesting dry conditions through this time, and it is possible that weak SWW flow between 11 and 9 ka resulted in enhanced aridity, desiccating any earlier organic deposition. From 9 ka onward, stronger westerly flow and moist conditions in the Western Cape region are suggested by an increase in the number of published organic sequences and is consistent with a review by Meadows and Baxter (1999), while a substantial decline in *Podocarpus* pollen toward a low at 5.5 ka reflects drying in the east, a pattern consistent with the effects of stronger SWW on precipitation in the modern climate (Fig. 1b), although it must be noted that this latter region lies in a summer-rainfall region, whereas westerly winds predominantly influence winter weather patterns in this region. The number of organic sequences changes little from 9 ka to the present in the Western Cape, while a marked drop in *Podocarpus* at 3 ka followed by an increase centred on 2 ka reveals variability in moisture regime on the southeast coast that may be attributable to changes in westerly flow.

6. Discussion

6.1. The Southern Westerly Winds since 14 ka

This synthesis, analysis, and reinterpretation of selected Southern Hemisphere palaeoenvironmental records represents the first attempt at integrating data from all Southern Hemisphere landmasses relevant to westerly wind changes in the post-LGM period. Despite the limited chronological control of many of the

records included in this analysis, there are clear near-synchronous and zonally symmetric multi-millennial trends in moisture balance in areas located within the modern SWW zone of influence over the last 14,000 years (Fig. 6). The pattern of correlations between westerly wind speed and precipitation in the modern climate of all Southern Hemisphere landmasses (Fig. 1b; Garreaud, 2007) provides a mechanistic framework with which to interpret long-term changes in relative moisture in terms of westerly wind influence. Although recognising that changes in the SWW may have been gradual and/or stepwise through time, five multi-millennial phases since 14 ka represent distinct phases of westerly wind strength and influence: 14–12, 11–8 ka, 7–5, 4–2, and 2–0 ka (Figs. 6 and 7).

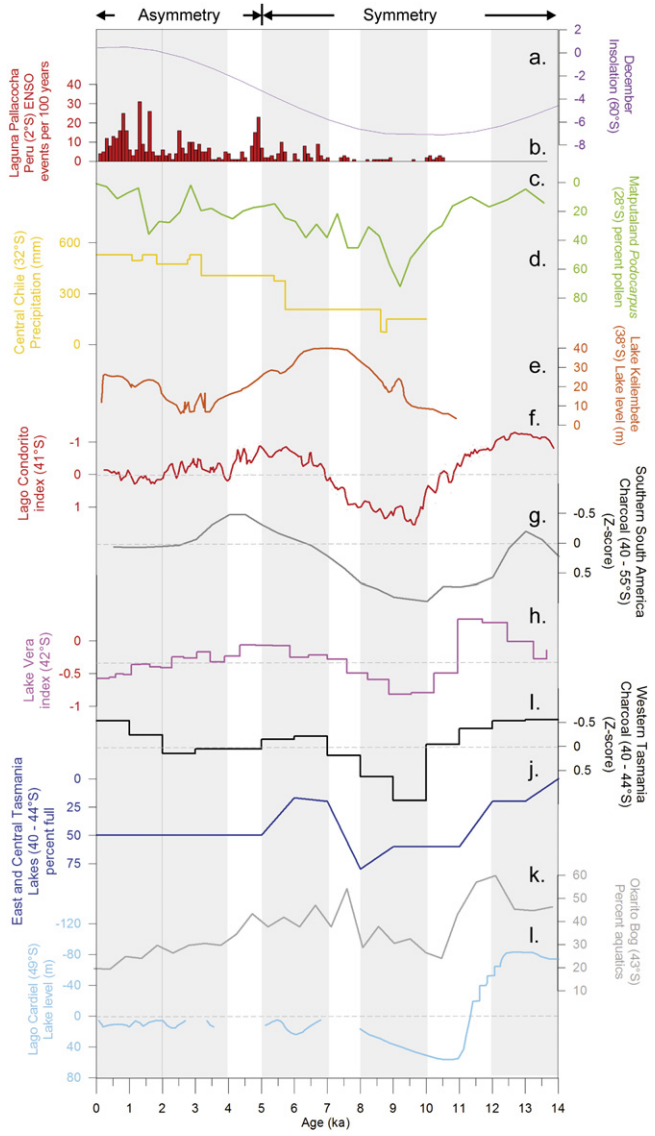

Fig. 6. Selected palaeoenvironmental data arranged in order of increasing latitude: (a) December insolation at 60°S (Berger, 1978); (b) Laguna Pallcacocha ENSO frequency (Moy et al., 2002); (c) Matputaland pollen record *Podocarpus* values (Site 1, Fig. 1a; Finch and Hill, 2008); (d) Laguna Aculeo precipitation curve (Site 10, Fig. 1a; Jenny et al., 2003); (e) Lake Keilambete lake-level curve (Site 4, Fig. 1a; Bowler and Hamada, 1971); (f) Lago Condorito palaeovegetation index (dashed line indicates the 14 ka mean) (Site 11, Fig. 1a; Moreno, 2004); (g) southern South American charcoal curve (dashed line indicates the 14 ka mean) (Power et al., 2008); (h) Lake Vera palaeovegetation index (dashed line indicates the 14 ka mean) (Site 7, Fig. 1a); (i) western Tasmanian regional charcoal curve (dashed line indicates the 14 ka mean) (Site 5, Fig. 1a; Fletcher and Thomas, 2010a); (j) eastern and central Tasmanian lake-level curve (Site 6, Fig. 1a; Harrison and Dodson, 1993); (k) Okarito Bog aquatic pollen content (Site 8, Fig. 1a; Newnham et al., 2007); (l) Lago Cardiel lake-level reconstruction (dashed line indicates the modern lake-level) (Site 12, Fig. 1a; Ariztegui et al., 2009). Note that the axes have been inverted for records located in zones that display a negative correlation between precipitation and westerly wind speed. See Fig. 1a for the location of sites.

6.1.1. Late Pleistocene to early Holocene (14–8 ka)

The latest Pleistocene (here 14–12 ka) represents the last stage of the global reorganisation of climate and biological systems to the rapid changes that characterised the Last Glacial Termination (Denton et al., 2010). Several glaciers in southern South America and New Zealand reached their maxima during an interval characterised by positive precipitation anomalies between 14 and 12 ka (Figs. 6 and 7), which in these regions are positively correlated with SWW strength (Fig. 1b). This was followed by a trend toward decreasing westerly wind influence at all sites (both north and south of the modern core of the SWW) between 11 and 8 ka across the entire westerly zone of influence (Figs. 6 and 7). The temporal offset between sites north and south of the modern westerly core in southern South America (Fig. 4e, f), the only landmass that intersects the westerlies through this zone, suggests an initial southward displacement of the westerlies at ~12.5 ka, followed by a weakening of the entire westerly wind belt after 11 ka (Moreno et al., 2010; Fletcher and Moreno, 2011)

In southern South America, moisture-driven vegetation changes and peak fire activity at a sub-continental scale occurs in pollen sequences from the hyper-humid regions of western Patagonia and Tierra del Fuego between 12.5 and 9.6 ka (Villagran, 1988; Heusser, 2003; Moreno, 2004; Massaferro et al., 2005; Villa-Martinez and Moreno, 2007; Whitlock et al., 2007; Abarzúa and Moreno, 2008; Power et al., 2008; Ponce et al., 2011), reflecting decreased SWW-derived moisture and weaker westerly flow (Moreno, 2004; Whitlock et al., 2007; Moreno et al., 2010; Fletcher and Moreno, 2011). Weak SWW flow over New Zealand during the early Holocene has been advocated as the driver of: (i) an expansion of frost and drought intolerant vegetation in the North Island (Shulmeister, 1999); (ii) the delayed post-glacial forest establishment on sub-Antarctic islands that lie below the modern westerly core (McGlone et al., 2000); (iii) a lack of glacial advances (Shulmeister et al., 2004); and (iv) increased moisture in the Otago region (Prebble and Shulmeister, 2002). Stratigraphic records from South Africa's Western Cape indicate a switch from wet to dry conditions during the late Pleistocene–early Holocene interval (Meadows and Baxter, 1999), concomitant with a change from dry to wet conditions in southeast southern Africa (Partridge, 1997) that is consistent with decreasing westerly influence over southern Africa through this time.

In contrast to the evidence presented above for decreasing influence of the SWW, several studies have postulated an increase in westerly influence from the late Pleistocene through to the early/mid Holocene in southern Australia (Harrison and Dodson, 1993; Donders et al., 2007), with the notion of an early Holocene increase/northward displaced westerlies entrenched in the Australian palaeoecological literature (e.g. Harrison, 1993; Dodson, 1998; Donders et al., 2007; Gingele et al., 2007; Moros et al., 2009). For example, an argument has been put forward for a uniform increase in moisture across southeast Australia during the early Holocene, resulting from a shift in the mean position of the high pressure belt that was driven by a warming trend and which resulted in increased westerly wind flow across the region (Donders et al., 2007). From first order principles, the modern relationship between westerly wind speed and the patterning of precipitation in southern Australia (Fig. 1b) argues against a uniform moisture increase across this vast and diverse region in response to stronger westerly flow. Rather, multi-millennial scale

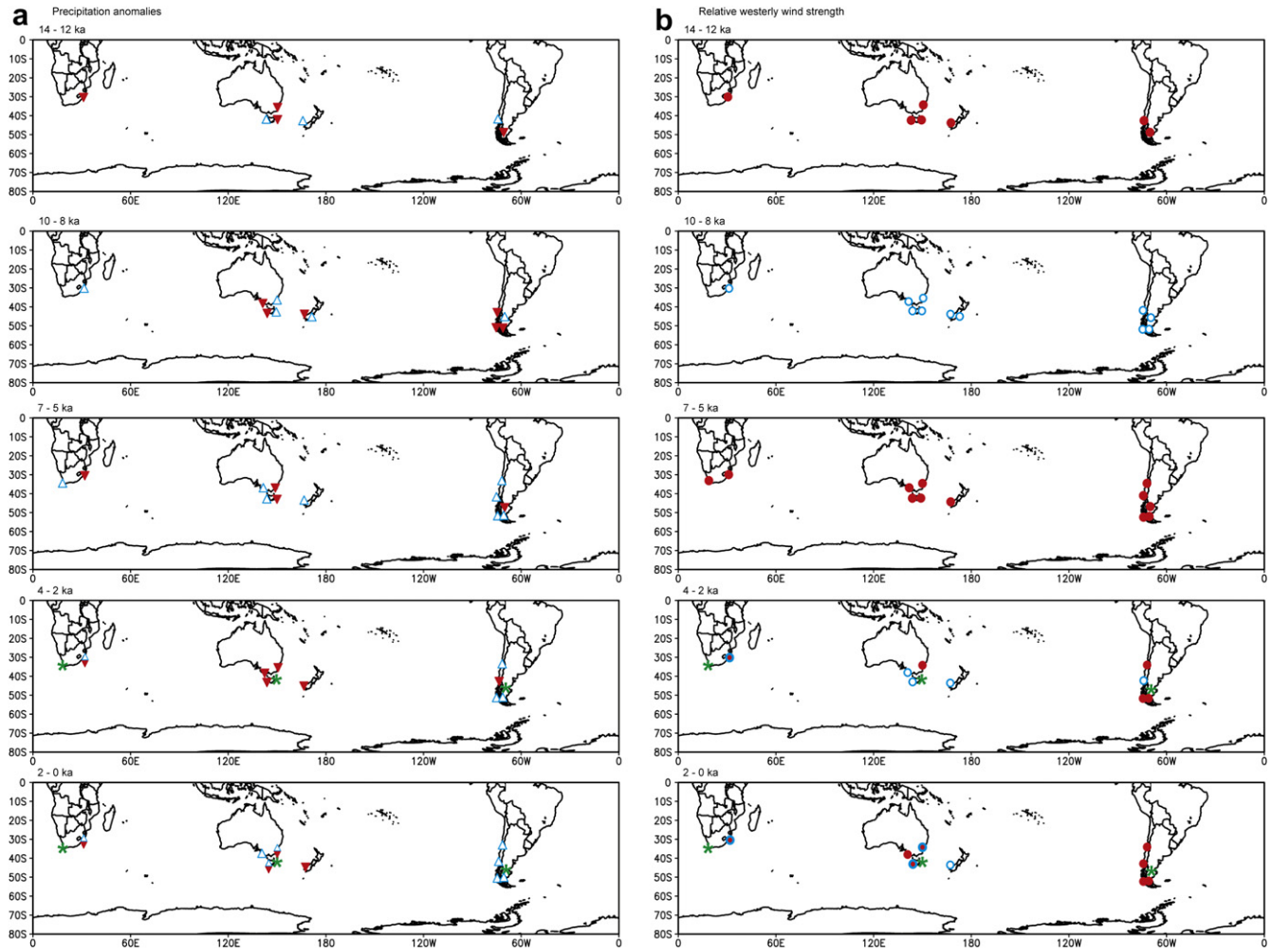

Fig. 7. Maps showing the reconstructed precipitation anomaly of sites analysed (a – left panel) and the inferred direction of SWW change (b – right panel) for the following time slices: 14–12 ka; 10–8 ka; 7–5 ka; 4–2 ka; and 2–0 ka. Red (blue) triangles in the precipitation anomaly maps indicate positive (negative) precipitation anomalies. Red (blue) circles in the relative SWW strength maps indicate stronger (weaker) westerly flow (For interpretation of the references to color in this figure legend, the reader is referred to the web version of this article.).

changes in westerly flow across this region would be expected to result in the east-west anti-phasing in moisture regimes observed in the modern climate (Fig. 1b). Furthermore, evidence for an invigorated and/or southward extension of the north Australian monsoon through the early Holocene (Johnson et al., 1999; Magee et al., 2004; Donders et al., 2007) stands in direct contrast to the notion of a simultaneous northward displacement or strengthening of the westerly wind belt.

Isolating moisture proxies from areas with precipitation regimes positively and negatively correlated with westerly wind speed has revealed that the modern east–west anti-phasing of precipitation regimes over southern Australia operates at multi-millennial timescales (Fig. 7) and that the period between ~12 and 8 ka was characterised by decreasing westerly influence over southern Australia. Moreover, this multi-millennial trend toward decreasing westerly flow between ~12 and 8 ka occurred on all southern landmasses, north and south of the modern core of the westerlies, displaying a clear zonal symmetry and implying a weakening and/or southward shift of atmospheric circulation though this time.

6.1.2. Mid Holocene (8–4 ka)

A zonally symmetric multi-millennial increase in westerly flow began by ~8 ka at most sites analysed here (Fig. 6), driving synchronous and zonally symmetric anti-phased moisture regime changes across all southern hemisphere landmasses, north and south of the current zone of maximum westerly wind speeds (McGlone et al., 2000; Moreno et al., 2010; Fletcher and Moreno, 2011; Ponce et al., 2011), reflecting an increase in westerly intensity (Moreno et al., 2010). In conjunction with a trend toward lower temperatures, this strengthening of the westerlies coincides with the onset of neoglaciation in southern South America and New Zealand (Moreno et al., 2009; Rojas and Moreno, 2010), bolstered by enhanced upwelling and northward advection of subpolar waters off the coast of Chile during the mid Holocene (Kaiser et al., 2008) and a steepening of the trans-Pacific SST gradient toward 7–6 ka in the equatorial Pacific Ocean (Koutavas et al., 2006). This steepening of the trans-Pacific SST would, consequently, set up conditions in which an enhanced Walker Cell circulation and more frequent ENSO events would prevail (sensu Shulmeister 1999; Koutavas et al., 2006). This scenario is consistent with a reconstruction of ENSO frequency that records an intensification of ENSO after ~6 ka (Fig. 6b; Moy et al., 2002).

6.1.3. Late Holocene (~4–0 ka)

The development of regional, zonal and meridional heterogeneities after 5 ka was detected in all the sectors under analysis (Figs. 6 and 7). For example, an apparently incoherent pattern is

evident in the multi-millennial trend toward lower moisture in northwest Patagonia (41°S), in opposition to an increase in moisture in central Chile (33°S) and Southwest Patagonia and Tierra del Fuego (52°S) after 5 ka. These trends were coeval with low lake-levels in southeast Australia (28°S) and southwest Victoria (35°S) and decreasing moisture in western Tasmania (41°S), a patterning inconsistent with the relationship between the SWW and precipitation in the modern climate of southern Australia (Figs. 1b). South of the modern core of the SWW, a multi-millennial increase in moisture at Lago Guanaco and Laguna Potrok Aike implies increasing westerly influence in that region through the late Holocene that is consistent with arguments for increased westerly flow after 5 ka over New Zealand (McGlone et al., 1993; Shulmeister, 1999; Shulmeister et al., 2004), yet is at odds with the decrease in aquatic pollen content at Okarito Bog (Figs. 6) and while it is possible that the Okarito Bog aquatic pollen content reflects authigenic processes on the mire surface at this time, rather than regional climate forcing, the complex and regionally heterogeneous trends in moisture across the Southern Hemisphere after ~5 ka signals a departure from the marked zonal symmetry of the proceeding period (14–5 ka), implying that multi-millennial moisture balances were modulated by factors other than zonally symmetric westerly changes.

6.2. Possible mechanisms

6.2.1. Insolation-driven westerly change?

Precessional-scale changes in solar insolation are the most commonly invoked driver of multi-millennial scale changes in atmospheric circulation, via their effect on meridional temperature gradients (e.g. Harrison and Dodson, 1993; Dodson, 1998; Magee et al., 2004; Cruz et al., 2005; Gilli et al., 2005a, 2005b; Donders et al., 2007), although which component of insolation drives global circulation is far from clear. Palaeoenvironmental data have been used to support hypotheses of both inter- and intra-seasonal insolation gradients to explain changes in the SWW over and since the LGM (Harrison and Dodson, 1993; Dodson et al., 1998; Shulmeister et al., 2004). Our results tentatively support the notion of an inter-seasonal driver of multi-millennial scale changes in the position and/or intensity of the SWW over the last 14,000 years, with a close relationship apparent between December insolation at 60°S (a proxy for the inter-seasonal insolation gradient; Shulmeister et al., 2004) and trends in westerly wind-driven moisture balances between 14 and 5 ka (Fig. 6a.). The apparent breakdown in the relationship between insolation and moisture balances after ~5 ka may reflect the dominance of climate modes not directly related to precessional-scale insolation, such as ENSO, the Southern Annular Mode, or the Pacific Decadal Oscillation of the Pacific-South American Mode.

6.2.2. A mid to late Holocene ENSO signal?

Two possible explanations are proposed for the development of regionally asymmetric trends in moisture balances of the southern landmasses after 5 ka: (1) a breakdown in the zonal symmetry of the SWW, or (2) the establishment of high-frequency precipitation variability resulting from more frequent ENSO oscillations since ~5 ka (Figs. 6b; Moy et al. 2002). The geographic patterning of multi-millennial moisture trends after ~5 ka (Figs. 6 and 7) is remarkably consistent with the modern expression of ENSO in the climate of the Southern Hemisphere (Power et al., 1999; Garreaud et al., 2009; Hill et al., 2009): the warm phase of ENSO (El Niño) results in the development of a strong high pressure cell below the southwest tip of southern South America that deflects the zonal westerlies north, resulting in anomalously dry conditions in northwest Patagonia and anomalously wet conditions in central Chile (Garreaud et al., 2009); while an anomalously high pressure system develops over southern Australia resulting in dry conditions along the eastern seaboard of Australia and all of Tasmania (Power et al., 1999; Hill et al., 2009). Evidence for the onset of ENSO in the western tropical Pacific after ~5 ka (Shulmeister and Lees, 1995; Wanner et al., 2008) and in the eastern tropical Pacific after ~6 ka (Moy et al., 2002) supports this notion of ENSO driving the breakdown in zonal symmetry after ~6–5 ka in the extra-tropical regions analysed here.

The paucity of data from southern Africa in this analysis precludes discussion of multi-millennial drivers of climate change through this period in that region, although evidence indicates enhanced climate variability in the late Holocene (Tyson et al., 2000; Lee Thorp et al., 2001). Jerardino (1995) discusses the similarities between palaeoclimate records in southern South America and southern Africa over the last ~5000 and these findings, coupled with evidence of an ENSO influence over modern South African climate (Mason, 2001) and evidence for ENSO-like millennial-scale climate variability in southern Africa (Holmgren et al., 2003), altogether, suggest that ENSO may have played a part in this region also.

6.3. The Southern Westerly Winds and atmospheric CO_2

Toggweiler et al. (2006) proposed that the SWW play a central role in governing global atmospheric CO_2 content via wind-driven upwelling and ventilation of CO_2-rich deep waters in the Southern Ocean, a notion that has received considerable attention (e.g. Tschumi et al., 2008; Anderson et al., 2009; Sijp and England, 2009; Toggweiler, 2009; Moreno et al., 2010; Sijp et al., 2010; Fletcher and Moreno, 2011). In a recent synthesis of a number of selected Southern Hemisphere palaeoenvironmental records, Fletcher and Moreno (2011) argue for a southward displacement of the SWW at ~12.5 ka that initiated a phase of enhanced wind-driven oceanic upwelling at circumpolar sites located >52°S (Anderson et al., 2009), driving an increase in atmospheric CO_2 via enhanced ventilation of the Southern Ocean (Toggweiler et al., 2006; Toggweiler, 2009). This was followed by a weakening of westerly flow across the entire zone of westerly influence, as indicated by a cessation of westerly driven oceanic upwelling in the sub-polar Southern Ocean (Anderson et al., 2009), a reversal of the atmospheric CO_2 trend and negative westerly derived moisture north (Lago Condorito) and south (Lago Guanaco) of the modern westerly core, a notion supported by the ample evidence presented in the present paper and by palaeoenvironmental reconstructions from sub-Antarctic sites (>52°S) in New Zealand (McGlone et al., 2000, 2010), Southwest Patagonia (Fesq-Martin et al., 2004; Lamy et al. 2010), Tierra del Fuego (Heusser, 2003) and Isla de los Estados (Ponce et al., 2011) for decreased westerly flow between 11 and 8 ka, and by substantial evidence that changes in SWW intensity are at least as important as latitudinal displacements for driving CO_2 fluxes out of the deep ocean at high southern latitudes (Tschumi et al., 2008; Sijp and England, 2009; Sijp et al., 2010). The evidence for a multi-millennial increase in SWW flow after ~8 ka is consistent with the multi-millennial increase in atmospheric CO_2 content (EPICA, 2004) (see Moreno et al., 2010; Fletcher and Moreno, 2011) and which appears to be unaffected by the breakdown in zonal symmetry evident after ~5 ka at sites located above 50°S, suggesting that the onset of ENSO variability in the tropical and extra-tropical Pacific did not affect the SWW-Southern Ocean coupled system (sensu Fletcher and Moreno, 2011).

7. Conclusion

This synthesis and analysis represents the first attempt at reconstructing changes in the globally important Southern

Westerly Winds (SWW) since 14 ka based on palaeoenvironmental data from all Southern Hemisphere landmasses. This interval shows a clear multi-millennial zonal symmetry of SWW, which is greatest between 14 and 5 ka, with a striking degree of synchrony and co-variability that clearly mirrors the modern relationship between zonal westerly wind speed and precipitation across the Southern Hemisphere. A breakdown in zonal symmetry coincided with the onset of ENSO variability after ~6-5 ka, possibly reflecting the influence of insolation-driven changes on the pole to equator thermal gradient on atmospheric circulation. A steepened gradient at this time would have driven stronger westerly winds and a general increase in the intensity of atmospheric circulation which, in turn, may have driven changes in oceanic circulation that altered oceanic SST and SLP gradients, triggering intensified Walker Cell circulation and the onset of an ENSO-dominated climate. This interpretation of zonally symmetric changes in the westerlies through much of the last 14,000 years lends significant support to notions of a SWW driver of global atmospheric CO_2 content via wind-driven overturning and ventilation of the Southern Ocean. The data analysed here only allows hemisphere-wide comparison at multi-millennial timescales and focus now needs to be directed at developing high-resolution and precisely dated palaeoenvironmental records targeted in areas within the entire zone of westerly influence, north and south of ~50°S, that specifically accounts for and addresses the heterogeneous manner in which westerlies impact upon the climate of southern landmasses and which will allow comparisons of millennial and centennial scale trends.

Acknowledgements

M.-S.F. is funded by the Institute of Ecology and Biodiversity, Chile, and Fondecyt 3110180. P.I.M. is funded by Fondecyt 1080485, 1110612 and Iniciativa Científica Milenio P05-002, contract PFB-23. We would like to thank René Garreaud for discussions on the mechanics of Southern Hemisphere climate. Comments on an earlier draft of the manuscript by Peter Kershaw and two anonymous referees were much appreciated.

References

Abarzúa, A.M., Moreno, P.I., 2008. Changing fire regimes in the temperate rainforest region of southern Chile over the last 16,000 yr. Quaternary Research 69 (1), 62–71.

Abarzúa, A.M., Villagran, C., Moreno, P.I., 2004. Deglacial and postglacial climate history in east-central Isla Grande de Chiloe, southern Chile (43° S). Quaternary Research 62, 49–59.

Anderson, B., Mackintosh, A., 2006. Temperature change is the major driver of late-Glacial and Holocene glacier fluctuations in New Zealand. Geology 34 (2), 121.

Anderson, R.F., Ali, S., Bratmiller, L.I., Nielsen, S.H.H., Fleisher, M.Q., Anderson, B.E., Burkle, L.H., 2009. Wind-driven upwelling in the southern ocean and the deglacial rise in atmospheric CO_2. Science 323, 1443–1448.

Anselmetti, F.S., Ariztegui, D., De Batist, M., Gebhardt, A.C., Haberzettl, T., Niessen, F., Ohlendorf, C., Zolitschka, B., 2009. Environmental history of southern Patagonia unravelled by the seismic stratigraphy of Laguna Potrok Aike. Sedimentology 56 (4), 873–892.

Ariztegui, D., Gilli, A., Anselmetti, F.S., Goñi, R.A., Belardi, J.B., Espinosa, S., 2009. Lake-level changes in central Patagonia (Argentina): crossing environmental thresholds for Lateglacial and Holocene human occupation. Journal of Quaternary Science. doi:10.1002/jqs.1352.

Barrows, T.T., Lehman, S.J., Fifield, L.K., De Deckker, P., 2007. Absence of cooling in New Zealand and the adjacent ocean during the Younger Dryas chronozone. Science 318 (5847), 86.

Berger, A.L., 1978. Long-term variations of daily insolation and Quaternary climatic changes. Journal of the Atmospheric Sciences 35 (12), 2362–2367.

Bowler, J.M., Hamada, T., 1971. Late Quaternary stratigraphy and radiocarbon chronology of water level fluctuations in Lake Keilambete, Victoria. Nature 232, 330–332.

Bowman, D.M.J.S., 2000. Australian Rainforests: Islands of Green in a Land of Fire. Cambridge University Press, Cambridge.

Bradbury, J.P., 1986. Late Pleistocene and Holocene palaeolimnology of two mountain lakes in western Tasmania. Palaios 1, 318–388.

Brugam, R.B., McCance Johnson, S., 1997. Holocene lake-level rise in the Upper Peninsula of Michigan, USA, as indicated by peatland growth. The Holocene 7 (3), 355–359.

Cep, B., 1923. Variations in the level of Lake George, Australia. Nature 112, 918.

Cruz, F.W., Burns, S.J., Karmann, I., Sharp, W.D., Vuille, M., Cardoso, A.O., Ferrari, J.A., Dias, P.L.S., Viana, O., 2005. Insolation-driven changes in atmospheric circulation over the past 116,000 years in subtropical Brazil. Nature 434 (7029), 63–66.

Dale, M.B., Allison, L., Dale, P.E.R., 2010. A model for correlation within clusters and its use in pollen analysis. Community Ecology 11 (1), 51–58.

De Deckker, P., 1982. Late Quaternary ostracods from Lake George New South Wales. Alcheringa 6, 305–318.

Denton, G.H., Anderson, R.F., Toggweiler, J.R., Edwards, R.L., Schaefer, J.M., Putnam, A.E., 2010. The Last Glacial Termination. Science 328 (5986), 1652.

Denton, G.H., Hendy, C.H., 1994. Younger Dryas age advance of Franz Josef glacier in the southern alps of New Zealand. Science 264 (5164), 1434.

Dixie, L.F., 1881. Across Patagonia. R. Worthington, London.

Dodson, J.R., 1998. Timing and response of vegetation change to Milankovitch forcing in temperate Australia and New Zealand. Global and Planetary Change 18 (3–4), 161–174.

Dodson, J.R., Mitchell, F.J.G., Bogeholz, H., Julian, N., 1998. Dynamics of temperate rainforest from fine resolution pollen analysis, Upper Ringarooma River, northeastern Tasmania. Australian Journal of Ecology 23, 550–561.

Donders, T.H., Haberle, S., Hope, G., Wagner, F., Visscher, H., 2007. Pollen evidence for the transition of the Eastern Australian climate system from the post-glacial to the present-day ENSO mode. Quaternary Science Reviews 26, 1621–1637.

Eeley, H.A.C., Lawes, M.J., Piper, S.E., 1999. The influence of climate change on the distribution of indigenous forest in KwaZulu-Natal, South Africa. Journal of Biogeography 26 (3), 595–617.

EPICA, 2004. Eight glacial cycles from an Antarctic ice core. Nature 429, 623–628.

Fesq-Martin, M., Friedmann, A., Peters, M., Behrmann, J., Kilian, R., 2004. Late-glacial and Holocene vegetation history of the Magellanic rain forest in southwestern Patagonia, Chile. Vegetation History and Archaeobotany 13 (4), 249–255.

Finch, J.M., Hill, T.R., 2008. A late Quaternary pollen sequence from Mfabeni Peatland, South Africa: reconstructing forest history in Maputaland. Quaternary Research 70 (3), 442–450.

Fitzharris, B.B., Hay, J.E., Jones, P.D., 1992. Behaviour of New Zealand glaciers and atmospheric circulation changes over the past 130 years. The Holocene 2 (2), 97–106.

Fitzsimmons, K.E., Barrows, T.T., 2010. Holocene hydrologic variability in temperate southeastern Australia: an example from Lake George, New South Wales. The Holocene 20 (4), 585–597.

Fitzsimons, S.J., 1997. Late-glacial and early Holocene glacier activity in the Southern Alps, New Zealand. Quaternary International 38, 69–76.

Fletcher, M.-S., Moreno, P.I., 2011. Zonally symmetric changes in the strength and position of the Southern Westerlies drove atmospheric CO_2 variations over the past 14 ky. Geology 39 (5), 419–422.

Fletcher, M.-S., Thomas, I., 2010a. The origin and temporal development of an ancient cultural landscape. Journal of Biogeography 37 (11), 2183–2196.

Fletcher, M.-S., Thomas, I., 2010b. A quantitative late Quaternary temperature reconstruction from western Tasmania, Australia. Quaternary Science Reviews 29, 2351–2361.

Futyma, R.P., Miller, N.G., 1986. Stratigraphy and genesis of the Lake Sixteen peatland, northern Michigan. Canadian Journal of Botany 64 (12), 3008–3019.

Garreaud, R.D., 2007. Precipitation and circulation covariability in the extratropics. Journal of Climate 20 (18), 4789–4797.

Garreaud, R.D., Vuille, M., Compagnucci, R., Marengo, J., 2009. Present-day South American climate. Palaeogeography, Palaeoclimatology, Palaeoecology 281 (3–4), 180–195.

Gellatly, A.F., Chinn, T.J.H., Röthlisberger, F., 1988. Holocene glacier variations in New Zealand: a review. Quaternary Science Reviews 7 (2), 227–242.

Gentilli, J., 1972. Australian Climate Patterns. The Griffin Press, Adelaide.

Gilli, A., Anselmetti, F.S., Ariztegui, D., Beres, M., McKenzie, J.A., Markgraf, V., 2005a. Seismic stratigraphy, buried beach ridges and contourite drifts: the late Quaternary history of the closed Lago Cardiel basin, Argentina (49°S). Sedimentology 52 (1), 1–23.

Gilli, A., Ariztegui, D., Anselmetti, F.S., McKenzie, J.A., Markgraf, V., Hajdas, I., McCulloch, R.D., 2005b. Mid-Holocene strengthening of the Southern Westerlies in South America – sedimentological evidences from Lago Cardiel, Argentina (49°S). Global and Planetary Change 49 (1–2), 75–93.

Gingele, F., De Deckker, P., Norman, M., 2007. Late Pleistocene and Holocene climate of SE Australia reconstructed from dust and river loads deposited offshore the River Murray Mouth. Earth and Planetary Science Letters 255 (3–4), 257–272.

Haberle, S.G., Bennett, K.D., 2004. Postglacial formation and dynamics of North Patagonian rainforest in the Chonos Archipelago, Southern Chile. Quaternary Science Reviews 23 (23–24), 2433–2452.

Harrison, S.P., 1993. Late Quaternary lake-level changes and climates of Australia. Quaternary Science Reviews 12 (4), 211–231.

Harrison, S.P., Dodson, J.R., 1993. Climates of Australia and New Guinea since 18,000 yr B.P. In: Wright Jr., H.E., Kutzbach, J.E., Webb III, T., Ruddiman, W.F., Street-Perrot, F.A., Bartlein, P.J. (Eds.), Global Climates Since the Last Glacial Maximum. University of Minnesota Press, Minneapolis, MN, pp. 265–293.

Hendon, H.H., Thompson, D.W.J., Wheeler, M.C., 2007. Australian rainfall and surface temperature variations associated with the Southern Hemisphere annular mode. Journal of Climate 20 (11), 2452–2467.

Hesse, P.P., Magee, J.W., van der Kaars, S., 2004. Late Quaternary climates of the Australian arid zone: a review. Quaternary International 118, 87–102.
Heusser, C.J., 1989a. Letter to the editor: Southern Westerlies during the Last Glacial Maximum. Quaternary Research 31, 423–425.
Heusser, C.J., 1989b. Polar perspective of late-Quaternary climates in the Southern Hemisphere. Quaternary Research 32 (1), 60–71.
Heusser, C.J., 2003. Ice Age Southern Andes: A Chronicle of Paleoecological Events. Elsevier Science.
Hill, K.J., Santoso, A., England, M.H., 2009. Interannual Tasmanian rainfall variability associated with large-scale climate modes. Journal of Climate 22, 4383–4397.
Holmgren, K., Lee-Thorp, J.A., Cooper, G.R.J., Lundblad, K., Partridge, T.C., Scott, L., Sithaldeen, R., Siep Talma, A., Tyson, P.D., 2003. Persistent millennial-scale climatic variability over the past 25,000 years in Southern Africa. Quaternary Science Reviews 22 (21–22), 2311–2326.
Huber, U.M., Markgraf, V., 2003. European impact on fire regimes and vegetation dynamics at the steppe-forest ecotone of southern Patagonia. The Holocene 13 (4), 567–579.
Huber, U.M., Markgraf, V., Schäbitz, F., 2004. Geographical and temporal trends in late Quaternary fire histories of Fuego-Patagonia, South America. Quaternary Science Reviews 23 (9–10), 1079–1097.
Huntington, M.A.M., Libbey, W., Morris, F., Brigham, A.P., Stevenson, E.L., 1908. Lake George, Australia. Bulletin of the American Geographical Society 40 (4), 217–220.
Jennings, J., 1981. The rise and fall of Lake George. Geographical Journal 53, 852–858.
Jenny, B., Valero-Garcés, B.L., Villa-Martínez, R., Urrutia, R., Geyh, M., Veit, H., 2002. Early to mid-Holocene aridity in Central Chile and the Southern Westerlies: the Laguna Aculeo record (34 S). Quaternary Research 58 (2), 160–170.
Jenny, B., Wilhem, D., Valero-Garces, B.L., 2003. The Southern Westerlies in Central Chile: Holocene precipitation estimates based on a water balance model for Laguna Aculeo (33°50′S). Climate Dynamics 20, 269–280.
Jerardino, A., 1995. Late Holocene Neoglacial episodes in southern South America and southern Africa: a comparison. The Holocene 5, 361–368.
Johnson, B.J., Miller, G.H., Fogel, M.L., Magee, J.W., Gagan, M.K., Chivas, A.R., 1999. 65,000 years of vegetation change in central Australia and the Australian summer monsoon. Science 284 (5417), 1150.
Jones, R.N., Bowler, J.M., McMahon, T.A., 1998. A high resolution Holocene record of P/E ratio from closed lakes in Western Victoria. Palaeoclimates 3, 51–82.
Kaiser, J., Schefuß, E., Lamy, F., Mohtadi, M., Hebbeln, D., 2008. Glacial to Holocene changes in sea surface temperature and coastal vegetation in north central Chile: high versus low latitude forcing. Quaternary Science Reviews 27 (21–22), 2064–2075.
Korhola, A., 1995. Holocene climatic variations in southern Finland reconstructed from peat-initiation data. The Holocene 5 (1), 43–57.
Koutavas, A., Demenocal, P.B., Olive, G.C., Lynch-Stieglitz, J., 2006. Mid-Holocene El Niño–Southern Oscillation (ENSO) attenuation revealed by individual foraminifera in eastern tropical Pacific sediments. Geology 34 (12), 993–996.
Lamy, F., Hebbeln, D., Wefer, G., 1999. High-resolution marine record of climatic change in Mid-latitude Chile during the last 28,000 years based on terrigenous sediment parameters. Quaternary Research 51 (1), 83–93.
Lamy, F., Kilian, R., Arz, H.W., Francois, J.P., Kaiser, J., Prange, M., Steinke, T., 2010. Holocene changes in the position and intensity of the southern westerly wind belt. Nature Geoscience, 695–699.
Latorre, C., Moreno, P.I., Vargas, G., Maldonado, A., Villa-Martínez, R., Armesto, J.J., Villagrán, C., Pino, M., Núñez, L., Grosjean, M., 2007. Late Quaternary environments and palaeoclimate. In: Moreno, T., Gibbons, W. (Eds.), The Geology of Chile. The Geological Society Publishing House, Bath, pp. 309–328.
Lee Thorp, J.A., Holmgren, K., Lauritzen, S.E., Linge, H., Moberg, A., Partridge, T.C., Stevenson, C., Tyson, P.D., 2001. Rapid climate shifts in the southern African interior throughout the mid to late Holocene. Geophysical Research Letters 28 (23), 4507–4510.
Lowell, T.V., Heusser, C.J., Andersen, B.G., Moreno, P.I., Hauser, A., Heusser, L.E., Schluchter, C., Marchant, D.R., Denton, G.H., 1995. Interhemispheric correlation of late Pleistocene glacial events. Science 269 (5230), 1541–1549.
Macphail, M.K., 1979. Vegetation and climates in southern Tasmania since the last glaciation. Quaternary Research 11, 306–341.
Magee, J.W., Miller, G.H., Spooner, N.A., Questiaux, D., 2004. Continuous 150 ky monsoon record from Lake Eyre, Australia: insolation-forcing implications and unexpected Holocene failure. Geology 32 (10), 885–888.
Mancini, M.V., Prieto, A.R., Paez, M.M., Schäbitz, F., Rabassa, J., 2008. Late Quaternary vegetation and climate of Patagonia. In: Developments in Quaternary Science, vol. 11. Elsevier, pp. 351–367.
Markgraf, V., 1987. Paleoenvironmental changes at the northern limit of the subantarctic Nothofagus forest, lat 37° S, Argentina. Quaternary Research 28 (1), 119–129.
Markgraf, V., 1989. Reply to CJ Heusser's "Southernwesterlies during the last glacial maximum." Quaternary Research 31 (3), 426–432.
Markgraf, V., 1993. Climatic history of Central and South America since 18 000 yr BP: comparison of pollen records and model simulations. In: Wright Jr., H.E., Kutzbach, J.E., Webb III, T., Ruddiman, W.F., Street-Perrot, F.A., Bartlein, P.J. (Eds.), Global Climates Since the Last Glacial Maximum. University of Minnesota Press, Minneapolis, MN, pp. 357–385.
Markgraf, V., Baumgartner, T.R., Bradbury, J.P., Diaz, H.F., 2000. Paleoclimate reconstruction along the Pole–Equator–Pole transect of the Americas (PEP 1). Quaternary Science Reviews 19 (1–5), 125–140.
Markgraf, V., Bradbury, J.P., Busby, J.R., 1986. Palaeoclimates in southwestern Tasmania during the last 13,000 years. Palios 1, 368–380.
Markgraf, V., Bradbury, J.P., Schwalb, A., Burns, S.J., Stern, C., Ariztegui, D., Gilli, A., Anselmetti, F.S., Stine, S., Maidana, N., 2003. Holocene palaeoclimates of southern Patagonia: limnological and environmental history of Lago Cardiel, Argentina. The Holocene 13, 581–591.
Markgraf, V., D'Antoni, H.L., Ager, T.A., 1981. Modern pollen dispersal in Argentina. Palynology 5, 43–63.
Markgraf, V., Dodson, J.R., Kershaw, P.A., McGlone, M.S., Nicholls, N., 1992. Evolution of late Pleistocene and Holocene climates in the circum-south pacific land areas. Climate Dynamics 6 (3–4), 193–211.
Markgraf, V., Huber, U.M., 2010. Late and postglacial vegetation and fire history in Southern Patagonia and Tierra del Fuego. Palaeogeography, Palaeoclimatology, Palaeoecology 297 (2), 351–366.
Markgraf, V., Whitlock, C., Haberle, S., 2007. Vegetation and fire history during the last 18,000 cal yr BP in Southern Patagonia: Mallín Pollux, Coyhaique, Province Aisén (45° 41′30″S, 71° 50′30″W, 640 m elevation). Palaeogeography, Palaeoclimatology, Palaeoecology 254 (3–4), 492–507.
Mason, S.J., 2001. El Niño, climate change, and Southern African climate. Environmetrics 12 (4), 327–345.
Massaferro, J., Brooks, S.J., Haberle, S.G., 2005. The dynamics of chironomid assemblages and vegetation during the late Quaternary at Laguna Facil, Chonos Archipelago, southern Chile. Quaternary Science Reviews 24 (23–24), 2510–2522.
Massaferro, J.I., Moreno, P.I., Denton, G.H., Vandergoes, M., Dieffenbacher-Krall, A., 2009. Chironomid and pollen evidence for climate fluctuations during the Last Glacial Termination in NW Patagonia. Quaternary Science Reviews 28 (5–6), 517–525.
McCarthy, A., Mackintosh, A., Rieser, U., Fink, D., 2008. Mountain glacier chronology from Boulder Lake, New Zealand, Indicates MIS 4 and MIS 2 Ice Advances of Similar Extent. Arctic, Antarctic, and Alpine Research 40 (4), 695–708.
McGlone, M.S., Moar, N.T., 1998. Dryland Holocene vegetation history, Central Otago and the Mackenzie Basin, South Island, New Zealand. New Zealand Journal of Botany 36 (1), 91–111.
McGlone, M.S., Salinger, M.J., Moar, N.T., Kutzbach, J.E., Webb III, T., Ruddiman, W.F., Street-Perrott, F.A., Bartlein, P.J., 1993. Paleovegetation studies of New Zealand's climate since the last glacial maximum. In: Wright Jr., H.E., Kutzbach, J.E., Webb III, T., Ruddiman, W.F., Street-Perrot, F.A., Bartlein, P.J. (Eds.), Global Climates Since the Last Glacial Maximum. University of Minnesota Press, Minneapolis, MN, pp. 294–317.
McGlone, M.S., Turney, C.S.M., Wilmshurst, J.M., Renwick, J., Pahnke, K., 2010. Divergent trends in land and ocean temperature in the Southern Ocean over the past 18,000 years. Nature Geoscience 3 (9), 622–626.
McGlone, M.S., Wilmshurst, J.M., Wiser, S.K., 2000. Lateglacial and Holocene vegetation and climatic change on Auckland Island, subantarctic New Zealand. The Holocene 10 (6), 719–728.
McWethy, D.B., Whitlock, C., Wilmshurst, J.M., McGlone, M.S., Li, X., 2009. Rapid deforestation of South Island, New Zealand, by early Polynesian fires. The Holocene 19 (6), 883–897.
Meadows, M.E., 1988. Late Quaternary peat accumulation in southern Africa. Catena 15 (5), 459–472.
Meadows, M.E., Baxter, A.J., 1999. Late Quaternary palaeoenvironments of the southwestern Cape, South Africa: a regional synthesis. Quaternary International 57, 193–206.
Meadows, M.E., Baxter, A.J., 2001. Holocene vegetation history and palaeoenvironments at Klaarfontein Springs, Western Cape, South Africa. The Holocene 11 (6), 699–706.
Meadows, M.E., Baxter, A.J., Parkington, J., 1996. Late Holocene environments at Verlorenvlei, Western Cape Province, South Africa. Quaternary International 33, 81–95.
Meadows, M.E., Sugden, J.M., 1991. A vegetation history of the last 14,000 years on the Cederberg, south-western Cape Province. South African Journal of Science 87 (1), 34–43.
Middleton, J.F., Bye, J.A.T., 2007. A review of the shelf-slope circulation along Australia's southern shelves: Cape Leeuwin to Portland. Progress in Oceanography 75 (1), 1–41.
Moreno, P.I., 2004. Millennial-scale climate variability in northwest Patagonia over the last 15000 yr. Journal of Quaternary Science 19 (1), 35–47.
Moreno, P.I., Francois, J.P., Moy, C.M., Villa-Martinez, R., 2010. Covariability of the Southern Westerlies and atmospheric CO_2 during the Holocene. Geology 38 (8), 727–730.
Moreno, P.I., Francois, J.P., Villa-Martinez, R.P., Moy, C.M., 2009. Millennial-scale variability in Southern Hemisphere westerly wind activity over the last 5000 years in SW Patagonia. Quaternary Science Reviews 28 (1–2), 25–38.
Moreno, P.I., Leon, A.L., 2003. Abrupt vegetation changes during the last glacial to Holocene transition in mid-latitude South America. Journal of Quaternary Science 18 (8), 787–800.
Moreno, P.I., Lowell, T.V., Jacobson, G.L., Denton, G.H., 1999. Abrupt vegetation and climate changes during the last glacial maximum and last termination in the Chilean Lake District: A case study from Canal de la Puntilla (41° S). Geografiska Annaler Series A: Physical Geography 81A (2), 285–311.
Moros, M., De Deckker, P., Jansen, E., Perner, K., Telford, R.J., 2009. Holocene climate variability in the Southern Ocean recorded in a deep-sea sediment core off South Australia. Quaternary Science Reviews 28, 1932–1940.

Moy, C.M., Dunbar, R.B., Moreno, P.I., Francois, J.P., Villa-Martinez, R., Mucciarone, D.M., Guilderson, T.P., Garreaud, R.D., 2008. Isotopic evidence for hydrologic change related to the westerlies in SW Patagonia, Chile, during the last millennium. Quaternary Science Reviews 27 (13–14), 1335–1349.

Moy, C.M., Seltzer, G.O., Rodbell, D.T., Anderson, D.M., 2002. Variability of El Nino/Southern Oscillation activity at millennial timescales during the Holocene. Nature 420, 162–165.

Mucina, L., Rutherford, M.C., 2006. The Vegetation of South Africa, Lesotho and Swaziland.

Newnham, R.M., Vandergoes, M.J., Hendy, C.H., Lowe, D.J., Preusser, F., 2007. A terrestrial palynological record for the last two glacial cycles from south-western New Zealand. Quaternary Science Reviews 26 (3–4), 517–535.

Nicholson, S.E., Flohn, H., 1980. African environmental and climatic changes and the general atmospheric circulation in late Pleistocene and Holocene. Climatic Change 2 (4), 313–348.

Ono, Y., Shulmeister, J., Lehmkuhl, F., Asahi, K., Aoki, T., 2004. Timings and causes of glacial advances across the PEP-II transect (East-Asia to Antarctica) during the last glaciation cycle. Quaternary International 118–119, 55–68.

Paez, M.M., Schäbitz, F., Stutz, S., 2001. Modern pollen-vegetation and isopoll maps in southern Argentina. Journal of Biogeography 28 (8), 997–1021.

Partridge, T.C., 1997. Cainozoic environmental change in southern Africa, with special emphasis on the last 200 000 years. Progress in Physical Geography 21 (1), 3–22.

Paruelo, J.M., Beltran, A., Jobbagy, E., Sala, O.E., Golluscio, R.A., 1998. The climate of Patagonia: general patterns and controls on biotic processes. Ecología Austral 8 (2), 85–101.

Ponce, J.F., Borromei, A.M., Rabassa, J.O., Martinez, O., 2011. Late Quaternary palaeoenvironmental change in western Staaten Island (54.5°S, 64°W), Fuegian Archipelago. Quaternary International 233, 89–100.

Power, M.J., Marlon, J., Ortiz, N., Bartlein, P.J., Harrison, S.P., Mayle, F.E., Ballouche, A., Bradshaw, R.H.W., Carcaillet, C., Cordova, C., Mooney, S., Moreno, P.I., Prentice, I.C., Thonicke, K., Tinner, W., Whitlock, C., Zhang, Y., Zhao, Y., Ali, A.A., Anderson, R.S., Beer, R., Behling, H., Briles, C., Brown, K.J., Brunelle, A., Bush, M., Camill, P., Chu, G.Q., Clark, J., Colombaroli, D., Connor, S., Daniau, A.L., Daniels, M., Dodson, J., Doughty, E., Edwards, M.E., Finsinger, W., Foster, D., Frechette, J., Gaillard, M.J., Gavin, D.G., Gobet, E., Haberle, S., Hallett, D.J., Higuera, P., Hope, G., Horn, S., Inoue, J., Kaltenrieder, P., Kennedy, L., Kong, Z.C., Larsen, C., Long, C.J., Lynch, J., Lynch, E.A., McGlone, M., Meeks, S., Mensing, S., Meyer, G., Minckley, T., Mohr, J., Nelson, D.M., New, J., Newnham, R., Noti, R., Oswald, W., Pierce, J., Richard, P.J.H., Rowe, C., Goni, M.F.S., Shuman, B.N., Takahara, H., Toney, J., Turney, C., Urrego-Sanchez, D.H., Umbanhowar, C., Vandergoes, M., Vanniere, B., Vescovi, E., Walsh, M., Wang, X., Williams, N., Wilmshurst, J., Zhang, J.H., 2008. Changes in fire regimes since the Last Glacial Maximum: an assessment based on a global synthesis and analysis of charcoal data. Climate Dynamics 30 (7–8), 887–907.

Power, S., Casey, T., Folland, C., Colman, A., Mehta, V., 1999. Inter-decadal modulation of the impact of ENSO on Australia. Climate Dynamics 15 (5), 319–324.

Prebble, M., Shulmeister, J., 2002. An analysis of phytolith assemblages for the quantitative reconstruction of late Quaternary environments of the Lower Taieri Plain, Otago, South Island, New Zealand. II: paleoenvironmental reconstruction. Journal of Paleolimnology 27 (4), 415–427.

Purdie, H., Mackintosh, A., Lawson, W., Anderson, B., 2011. Synoptic influences on snow accumulation on glaciers east and west of a topographic divide: Southern Alps, New Zealand. Arctic, Antarctic, and Alpine Research 43 (1), 82–94.

Read, J., Busby, J.R., 1990. Comparative responses to temperature of the major canopy species of Tasmanian cool temperate rainforest and their ecological significance. II. Net photosynthesis and climate analysis. Australian Journal of Botany 38 (2), 185–205.

Rojas, M., Moreno, P.I., 2010. Atmospheric circulation changes and neoglacial conditions in the Southern Hemisphere mid-latitudes: insights from PMIP2 simulations at 6 kyr. Climate Dynamics. doi:10.1007/s00382-010-0866-3.

Rojas, M., Moreno, P.I., Kageyama, M., Crucifix, M., Hewitt, C., Abe-Ouchi, A., Ohgaito, R., Brady, E.C., Hope, P., 2009. The Southern Westerlies during the Last Glacial Maximum in PMIP2 simulations. Climate Dynamics 32 (4), 525–548.

Schaefer, J.M., Denton, G.H., Kaplan, M., Putnam, A., Finkel, R.C., Barrell, D.J.A., Andersen, B.G., Schwartz, R., Mackintosh, A., Chinn, T., Schluchter, C., 2009. High-frequency Holocene glacier fluctuations in New Zealand differ from the northern signature. Science 324 (5927), 622–625.

Schalke, H., 1973. The upper Quaternary of the Cape Flats area (Cape Province, South Africa). Scripta Geologica 15, 1–57.

Shulmeister, J., 1999. Australasian evidence for mid-Holocene climate change implies precessional control of Walker Circulation in the Pacific. Quaternary International 57, 81–91.

Shulmeister, J., Fink, D., Hyatt, O.M., Thackray, G.D., Rother, H., 2010. Cosmogenic Be-10 and Al-26 exposure ages of moraines in the Rakaia Valley, New Zealand and the nature of the last termination in New Zealand glacial systems. Earth and Planetary Science Letters 297 (3–4), 558–566.

Shulmeister, J., Goodwin, I., Renwick, J., Harle, K., Armand, L., McGlone, M.S., Cook, E.J., Dodson, J.R., Mayewski, P., Curran, M., 2004. The Southern Hemisphere westerlies in the Australasian sector over the last glacial cycle: a synthesis. Quaternary International 118–119, 23–53.

Shulmeister, J., Lees, B.G., 1995. Pollen evidence from tropical Australia for the onset of an ENSO-dominated climate at c. 4000 BP. The Holocene 5 (1), 10–18.

Sijp, W.P., England, M.H., 2009. Southern Hemisphere westerly wind control over the ocean's thermohaline circulation. Journal of Climate 22 (5), 1277–1286.

Sijp, W.P., England, M.H., Meissner, K.J., 2010. On the control of glacial–interglacial atmospheric CO_2 variations by the Southern Hemisphere westerlies. Geophysical Research Letters 37 (21), L21703.

Singh, G., Geissler, E.A., 1985. Late Cainozoic history of vegetation, fire, lake levels and climate, at Lake George, New South Wales, Australia. Philosophical Transactions of the Royal Society of London. Series B: Biological Sciences 311 (1151), 379–447.

Singh, G., Kershaw, P., Clark, R.L., 1981. Quaternary vegetation and fire history in Australia. In: Gill, A.M., Groves, R.H., Noble, I.R. (Eds.), Fire and the Australian Biota. Australian Academy of Science, Canberra, pp. 23–54.

Street-Perrott, F.A., Perrott, R.A., 1993. Holocene vegetation, lake levels and climate of Africa. In: Wright Jr., H.E., Kutzbach, J.E., Webb III, T., Ruddiman, W.F., Street-Perrot, F.A., Bartlein, P.J. (Eds.), Global Climates Since the Last Glacial Maximum. University of Minnesota Press, Minneapolis, MN, pp. 318–356.

Stuiver, M., Reimer, P.J., Reimer, R., 2010. CALIB Radiocarbon Calibration Version 6.0.1 Available Online.

Sturman, A.P., Tapper, N.J., 2006. The Weather and Climate of Australia and New Zealand. Oxford University Press, USA.

Toggweiler, J.R., 2009. Climate change: shifting westerlies. Science 323 (5920), 1434.

Toggweiler, J.R., Russell, J.L., Carson, S.R., 2006. Midlatitude westerlies, atmospheric CO_2, and climate change during the ice ages. Paleoceanography 21, PA2005.

Tschumi, T., Joos, F., Parekh, P., 2008. How important are Southern Hemisphere wind changes for low glacial carbon dioxide? A model study. Paleoceanography 23 (26), 4208.

Tuhkanen, S., 1992. The climate of Tierra del Fuego from a vegetation geographical point of view and its ecoclimatic counterparts elsewhere. Acta Botanica Fennica 145, 1–64.

Tuhkanen, S., Kuokka, I., Hyvönen, J., Stenroos, S., Niemelä, J., 1992. Tierra del Fuego as a target for biogeographical research in the past and present. Anales del Instituto de la Patagonia. Serie Ciencias Naturales 19, 1–107.

Turney, C.M., Kershaw, P., Lowe, J.J., van Der Kaars, S., Johnson, R., Rule, S., Moss, P., Radke, L., Tibby, J., McGlone, M.S., Wilmshurst, J.M., Vandergoes, M.J., Fitzsimons, S.J., Bryant, C., James, S., Branch, N.P., Cowley, J., Kalin, R.M., Ogle, N., Jacobsen, G., Fifield, L.K., 2006a. Climatic variability in the southwest Pacific during the Last Termination (20–10 kyr BP). Quaternary Science Reviews 25, 886–903.

Turney, C.S.M., Haberle, S., Fink, D., Kershaw, A.P., Barbetti, M., Barrows, T.T., Black, M., Cohen, T.J., Correge, T., Hesse, P.P., 2006b. Integration of ice-core, marine and terrestrial records for the Australian Last Glacial Maximum and Termination: a contribution from the OZ INTIMATE group. Journal of Quaternary Science 21 (7), 751–761.

Tyson, P.D., Karlén, W., Holmgren, K., Heiss, G.A., 2000. The Little Ice Age and medieval warming in South Africa. South African Journal of Science 96 (3), 121–126.

Tyson, P.D., Preston-Whyte, R.A., 2000. The Weather and Climate of Southern Africa. Oxford Univ Press.

Ummenhofer, C.C., England, M.H., 2007. Interannual extremes in New Zealand precipitation linked to modes of Southern Hemisphere climate variability. Journal of Climate 20 (21), 5418–5440.

Veblen, T.T., Markgraf, V., 1988. Steppe expansion in Patagonia. Quaternary Research 30, 331–338.

Veit, H., 1996. Southern Westerlies during the Holocene deduced from geomorphological and pedological studies in the Norte Chico, Northern Chile (27–33° S). Palaeogeography, Palaeoclimatology, Palaeoecology 123 (1–4), 107–119.

Villa-Martinez, R., Moreno, P.I., 2007. Pollen evidence for variations in the southern margin of the westerly winds in SW Patagonia over the last 12,600 years. Quaternary Research 68 (3), 400–409.

Villagran, C., 1988. Late Quaternary vegetation of southern Isla Grande de Chiloé, Chile. Quaternary Research 29 (3), 294–306.

Wanner, H., Beer, J., Bütikofer, J., Crowley, T.J., Cubasch, U., Flückiger, J., Goosse, H., Grosjean, M., Joos, F., Kaplan, J.O., 2008. mid- to late Holocene climate change: an overview. Quaternary Science Reviews 27 (19–20), 1791–1828.

Wardle, P., 1991. Vegetation of New Zealand. Cambridge Univ Press.

Weaver, A.J., Middleton, J.H., 1989. On the dynamics of the Leeuwin Current. Journal of Physical Oceanography 19 (5), 626–648.

Weckstrom, J.A.N., Seppä, H., Korhola, A., 2010. Climatic influence on peatland formation and lateral expansion in subarctic Fennoscandia. Boreas 39 (4), 761–769.

Whitlock, C., Moreno, P.I., Bartlein, P., 2007. Climatic controls of Holocene fire patterns in southern South America. Quaternary Research 68 (1), 28–36.

Wilmshurst, J.M., Anderson, A.J., Higham, T.F.G., Worthy, T.H., 2008. Dating the late prehistoric dispersal of Polynesians to New Zealand using the commensal Pacific rat. Proceedings of the National Academy of Sciences of United States of America 105 (22), 7676–7680.

Wyrwoll, K.H., Dong, B., Valdes, P., 2000. On the position of southern hemisphere westerlies at the Last Glacial Maximum: an outline of AGCM simulation results and evaluation of their implications. Quaternary Science Reviews 19 (9), 881–898.